

Conditional counting statistics of electrons tunneling through quantum dot systems measured by a quantum point contact

Yen-Jui Chang,^{1,2} Tsung-Kang Yeh,¹ Chao-Hung Wan,¹ D. Wahyu Utami,³ Gerard J. Milburn,⁴ and Hsi-Sheng Goan^{1,2,*}

¹*Department of Physics and Center for Theoretical Sciences, National Taiwan University, Taipei 10617, Taiwan*

²*Center for Quantum Science and Engineering, National Taiwan University, Taipei 10617, Taiwan*

³*Research Systems and Reporting, Australian Catholic University, North Sydney, NSW 2060, Australia*

⁴*Centre for Engineered Quantum Systems, School of Mathematics and Physics, The University of Queensland, St Lucia, QLD 4072, Australia*

(Received 18 July 2017; revised manuscript received 13 November 2017; published 29 November 2017)

We theoretically study the conditional counting statistics of electron transport through a system consisting of a single quantum dot (SQD) or coherently coupled double quantum dots (DQD's) monitored by a nearby quantum point contact (QPC) using the generating functional approach with the maximum eigenvalue of the evolution equation matrix method, the quantum trajectory theory method (Monte Carlo method), and an efficient method we develop. The conditional current cumulants that are significantly different from their unconditional counterparts can provide additional information and insight into the electron transport properties of mesoscopic nanostructure systems. The efficient method we develop for calculating the conditional counting statistics is numerically stable, and is capable of calculating the conditional counting statistics for a more complex system than the maximum eigenvalue method and for a wider range of parameters than the quantum trajectory method. We apply our method to investigate how the QPC shot noise affects the conditional counting statistics of the SQD system, going beyond the treatment and parameter regime studied in the literature. We also investigate the case when the interdot coherent coupling is comparable to the dephasing rate caused by the back-action of the QPC in the DQD system, in which there is considerable discrepancy in the calculated conditional current cumulants between the population rate (master-) equation approach of sequential tunneling and the full quantum master-equation approach of coherent tunneling.

DOI: [10.1103/PhysRevB.96.195440](https://doi.org/10.1103/PhysRevB.96.195440)

I. INTRODUCTION

The time-resolved measurement of electron charges through a single quantum dot (SQD) by a nearby quantum point contact (QPC) detector has been demonstrated experimentally [1–6]. The ability to detect individual charges in real time makes it possible to count electrons one by one as they pass through the quantum dot (QD) [1–11]. The time-resolved charge detection has allowed the precise measurement of the QD shot noise at subfemtoampere current levels, and the full counting statistics (FCS) of the current [4–6].

FCS in quantum transport provides information of quantum statistical properties of transport phenomena and is studied mostly based on the computation of its moment or cumulant generating function [12–14]. Computing the generating function is more convenient in practice than the direct calculation of the probability distribution function and then performing average over the powers of electron number or current. A theoretical approach called number-resolved master-equation approach has been applied to calculate the generating functions and unconditional FCS for the nanostructure electron transport problems [13–19].

When a measurement is made on a single quantum system and the result is available, the state or density matrix of the system is a conditional state conditioned on the measurement result [20–22]. Thus, the conditional state of the system is important when its subsequent time evolution is concerned. If a single system is under continuous monitoring and one wants to map out the system state evolution conditioned on the contin-

uous in time measurement results, the conditional (Bayesian) stochastic Schrödinger or stochastic master-equation approach or the quantum trajectory theory (quantum Monte Carlo method) can be employed [20–24]. Each quantum trajectory can mimic the stochastic system state evolution conditioned on the continuous in time measurement outcomes in a single run of a realistic experiment. The stochastic element in the quantum trajectory corresponds exactly to the consequence of the random outcomes of the measurement record [20–24]. Thus, the quantum trajectories have the full information of the statistical properties about the measured system and can give insight to the unconditional quantities.

In some cases, one is concerned with the system state or physical observables conditioned on some average quantities (e.g., average current) in a given period of time rather than instantaneous and continuous in time measurement results. For example, the conditional counting statistics of electron transport through a SQD coupling to a QPC has been measured in the experiment by Sukhorukov *et al.* [25]. The conditional FCS that is the statistical current cumulant of one system given the observation of a particular average current in time t in the other system could be substantially different from its unconditional counterpart. A theoretical approach that utilizes the number-resolved rate (master) equation of a bistable SQD system and neglects the QPC shot noise was put forward to calculate the steady-state conditional FCS for the SQD-QPC system [25,26].

One of the purposes of this paper is to provide a connection with, and a unified picture of, the quantum trajectory, the (partially reduced) number-resolved master equation, and the unconditional (reduced) master-equation approaches. We show that the master equations for the reduced or partially

*goan@phys.ntu.edu.tw

reduced density matrix can be simply obtained when an average or partial average is taken on the conditional, stochastic density matrix (or quantum trajectories) over the possible outcomes of the measurements [21–23].

Another purpose of this paper is to investigate the effect of QPC shot noise on the conditional FCS of the SQD-QPC system as well as to develop an efficient and systematic way to calculate the conditional FCS for more complex systems of interacting nanoscale conductors. Our investigation goes beyond the analysis presented in Ref. [25]. In Ref. [25], the number-resolved population master (rate) equation for bistable system was first transformed into the counting field (inverse Fourier transform) space and then the eigenvalue with the smallest absolute real part (or maximum eigenvalue) in the matrix of the transformed master equation was found analytically. To evaluate the integral in partial or mixed Fourier transform space analytically with the analytic form of the eigenvalue to obtain the conditional steady-state current moment (cumulant) generating function, a further approximation to neglect the QPC shot noise was made [25]. For the experimental parameters used in Ref. [25], the QPC shot noise as compared to the noise contribution of the random telegraph signal in the QPC current trace induced by random electrons tunneling on and off the QD is indeed small and can be neglected. On the other hand, for the parameter regimes where the QPC shot noise cannot be ignored, obtaining analytical expressions for the conditional steady-state current moments or cumulants is very difficult. Furthermore, for more complicated interacting nanoscale conductors with the dimension of the matrix equation of the master equation growing up, to find analytical solution of the maximum eigenvalue becomes very hard, not to mention to obtain the analytical forms of the conditional steady-state current moment or current cumulant generating function. Besides, direct numerical evaluation of the conditional cumulant generation function in the same way as in Ref. [25] and then taking partial derivatives to obtain conditional cumulants are quite numerically unstable. In these cases, the quantum trajectory approach may give the conditional states or conditional current cumulants by simultaneously simulating an ensemble of current outcomes and corresponding quantum trajectories, and then categorizing and averaging the current outcomes of one system (e.g., the QD system) for each of the observed average current values in the other system (e.g., the QPC). However, in some parameter regimes where the probabilities to observe the average QPC current in certain values are very small, it is then computationally expensive to simulate and map out the conditional current cumulant in the whole parameter space of the average QPC current by the quantum trajectory method as an extremely large number of trajectories are required to have enough statistical samples in those very low probability domains. Thus, developing a method to evaluate the conditional counting statistics directly and effectively for more complex systems and for a wide range of parameter space is desirable. It is one of the aims of the paper to develop such an efficient method.

The paper is organized as follows. In Sec. II, we introduced the model and Hamiltonian of the QD-QPC system that will be considered. In Sec. III, we present the unconditional master equation for the reduced density matrix of the QD system.

We then derive the conditional, stochastic master equation (or quantum trajectory equation) that mimics the dynamics of the QD system conditioned on the observed random outcomes in Sec. IV. Then, the number-resolved master equation and its inverse Fourier transform in the counting field space are discussed in Sec. V. The procedure to calculate the unconditional and conditional FCS are described in terms of generating functional approach in Sec. VI. Here, we also introduce our efficient method to calculate the moments and cumulants of the conditional FCS. Section VII is devoted to the presentation and discussion of the results we obtain. Specifically, we provide a thorough analysis using the method of Ref. [25], the quantum trajectory theory, and the efficient method we develop to simulate and calculate the conditional current and noise of the SQD-QPC and DQD-QPC systems. We also investigate how the QPC shot noise affects the conditional QD current cumulants. Finally, a short conclusion is given in Sec. VIII. The detailed procedure of the semiempirical method used to count the number of tunneling electrons through the QD system in each random current trace of quantum trajectories is described in the Appendix.

II. QUANTUM DOT SYSTEM MEASURED BY A QPC

We consider a system consisting of either a SQD [see Fig. 1(a)] or coherently coupled DQD's [Fig. 1(b)] measured by a QPC [4,5,15,25,27]. The QD system is connected to two leads (reservoirs) biased so that electrons can tunnel onto the SQD (onto the left dot of the coherently coupled DQD's) from the left lead and off the SQD (off the right dot of the DQD's) onto the right lead. The QPC serves as a sensitive electrometer since its tunneling barrier can be modulated by the charge on a nearby QD. In our setup, as the electron moves into the SQD (the right dot of the DQD's), it changes the tunnel barrier of the nearby QPC. In this way, the modulated current through the QPC can be used to continuously monitor the occupation of the QD. We will follow the treatment given in Refs. [21–23] to describe the dynamics of the system.

The Hamiltonian for the QD system coupling to the QPC can be written as

$$\mathcal{H} = \mathcal{H}_{\text{QD}} + \mathcal{H}_{\text{QPC}} + \mathcal{H}_{\text{coup}}, \quad (1)$$

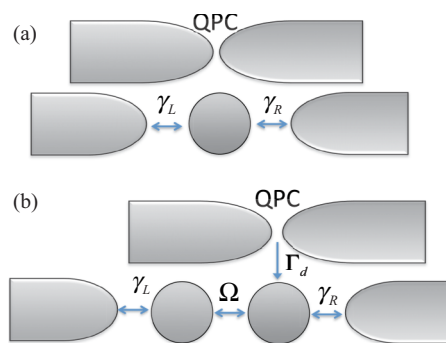


FIG. 1. Schematic illustration of (a) SQD and (b) coherently coupled DQD's connected to two Fermi reservoirs (left and right leads) by tunnel junctions, measured by a charge-sensitive QPC detector. Electrons tunneling through the QD modulate the tunneling current through the QPC.

where

$$\mathcal{H}_{\text{QD}} = H_S + \sum_k \hbar\omega_{Lk} a_{Lk}^\dagger a_{Lk} + \hbar\omega_{Rk} a_{Rk}^\dagger a_{Rk} + \sum_k t_{Lk} a_{Lk} c_i^\dagger + t_{Rk} a_{Rk} c_j^\dagger + \text{H.c.}, \quad (2)$$

$$\mathcal{H}_{\text{QPC}} = \hbar \sum_k (\omega_{sk} a_{sk}^\dagger a_{sk} + \omega_k^R a_{dk}^\dagger a_{dk}) + \sum_{k,q} (T_{kq} a_{sk}^\dagger a_{dq} + T_{qk}^* a_{dq}^\dagger a_{sk}), \quad (3)$$

$$\mathcal{H}_{\text{coup}} = \sum_{k,q} c_j^\dagger c_j (\chi_{kq} a_{sk}^\dagger a_{dq} + \chi_{qk}^* a_{dq}^\dagger a_{sk}), \quad (4)$$

where \mathcal{H}_{QD} here is the Hamiltonian for the QD system consisting of the left lead, right lead, and the central part system and the tunneling between them. The symbols a_{Lk} , a_{Rk} and $\hbar\omega_{Lk}$, $\hbar\omega_{Rk}$ are, respectively, the electron annihilation operators and energies for the left and right reservoir states for the QD system at wave number k . For a SQD system, we have the indices $i = j = 2$ in \mathcal{H}_{QD} and the Hamiltonian of the central part system is just

$$H_S = \hbar\omega_2 c_2^\dagger c_2, \quad (5)$$

and for a DQD system, we have $i = 1$, $j = 2$ in \mathcal{H}_{QD} and

$$H_S = \hbar\omega_1 c_1^\dagger c_1 + \hbar\omega_2 c_2^\dagger c_2 + \hbar\Omega(c_1^\dagger c_2 + c_2^\dagger c_1). \quad (6)$$

Here, c_j (c_j^\dagger) and $\hbar\omega_j$ represent the electron annihilation (creation) operator and energy for a single-electron state in dot j , respectively. In other words, dot 2 denotes the central QD in the SQD system, and dots 1 and 2 stand for the left dot and right dot, respectively, in the DQD system. The tunneling Hamiltonian for the QPC detector is represented by \mathcal{H}_{QPC} . Similarly, a_{sk} , a_{dk} and $\hbar\omega_{sk}$, $\hbar\omega_{dk}$ are, respectively, the electron annihilation operators and energies for the source and drain reservoir states for the QPC at wave number k . $\mathcal{H}_{\text{coup}}$ [Eq. (4)] describes the interaction between the QPC detector and dot $j = 2$. When the electron is located in dot $j = 2$, the effective tunneling amplitude of the QPC detector changes from $T_{kq} \rightarrow T_{kq} + \chi_{kq}$. We investigate here a simpler case of electrons transport through the DQD-QPC system in which the QPC couples only to the right dot (dot 2) of the DQD system [5,15,27,28] to illustrate the usage of our method and discuss the effects of QPC shot noise and interdot coupling on the conditional current cumulants. Our approach can be straightforwardly generalized to the case where the QPC couples to both dots with different coupling strengths [5,10,11,29–31].

III. UNCONDITIONAL MASTER EQUATION

By following the treatment in Refs. [15,21,22], the (unconditional) zero-temperature, Markovian master equation of the reduced density matrix for the quantum dot (QD) system can be obtained as

$$\dot{\rho}(t) = -\frac{i}{\hbar} [H_S, \rho(t)] + \gamma_L \mathcal{D}[c_i^\dagger] \rho(t) + \gamma_R \mathcal{D}[c_j] \rho(t) + \mathcal{D}[\mathcal{T} + \mathcal{X} n_j] \rho(t) \quad (7)$$

$$\equiv \mathcal{L} \rho(t), \quad (8)$$

where $n_j = c_j^\dagger c_j$ is the occupation number operator of dot j measured by the QPC. In Eq. (7) and the rest of the paper, the Hamiltonian of the QD system H_S takes the form of Eq. (5) for the SQD system and Eq. (6) for the DQD system, and the subscripts $i = j = 2$ for the SQD system and $i = 1$ and $j = 2$ for the DQD system. The parameters \mathcal{T} and \mathcal{X} are given by $D = |\mathcal{T}|^2 = 2\pi |T_{00}|^2 g_s g_d V / \hbar$, and $D' = |\mathcal{T} + \mathcal{X}|^2 = 2\pi |T_{00} + \chi_{00}|^2 g_s g_d V / \hbar$. Here, D and D' are the average electron tunneling rates through the QPC barrier without and with the presence of the electron in dot $j = 2$, respectively, $eV = \mu_s - \mu_d$ is the external bias applied across the QPC (μ_s and μ_d stand for the chemical potentials in the source and drain reservoirs, respectively), T_{00} and χ_{00} are energy-independent tunneling amplitudes near the average chemical potential, and g_s and g_d are the energy-independent density of states for the source and drain reservoirs. γ_L and γ_R are from the QD system to the right lead, respectively. In Eq. (7), the superoperator \mathcal{D} is defined as

$$\mathcal{D}[B] \rho = \mathcal{J}[B] \rho - \mathcal{A}[B] \rho, \quad (9)$$

where $\mathcal{J}[B] \rho = B \rho B^\dagger$, $\mathcal{A}[B] \rho = (B^\dagger B \rho + \rho B^\dagger B) / 2$. Finally, Eq. (8) defines the Liouvillian operator \mathcal{L} .

The conditional dynamics is quite different from its unconditional counterpart. For example, the unconditional dynamics of the number of electrons on the SQD system follows immediately from Eqs. (7) and (5) as

$$\frac{d\langle n_2 \rangle(t)}{dt} = \gamma_L [1 - \langle n_2 \rangle(t)] - \gamma_R \langle n_2 \rangle(t), \quad (10)$$

where $\langle n_2 \rangle(t) = \text{Tr}[c_2^\dagger c_2 \rho(t)]$. Clearly, the average current through the SQD does not depend at all on the current through the QPC in this model. This is because the Hamiltonian describing the interaction between the SQD and the QPC commutes with the number operator n_2 . However, if we ask for the conditional dynamics of the SQD *given* an observed averaged current in time t or *given* an instantaneous current in time dt through the QPC, we need a different equation or even a stochastic equation for $\langle n_2 \rangle_c$.

IV. CONDITIONAL MASTER EQUATION AND QUANTUM TRAJECTORIES

There are two classical stochastic currents through this system: the current $I(t)$ through the QPC and the current $J(t)$ through the QD. Equation (7) describes the time evolution of the reduced density matrix when these classical stochastic processes are averaged over. To make contact with a single realization of the random outcomes of the measurement records and study the stochastic evolution of the QD state, conditioned on a particular measurement realization, we need the conditional master equation. We first define the relevant point processes that are the source of the classically observed stochastic currents.

We specify the quantum-jump conditional dynamics through the QPC by defining the point processes [21–24]

$$[dN_c(t)]^2 = dN_c(t), \quad (11)$$

$$\begin{aligned} E[dN_c(t)] &= \zeta \text{Tr}[\tilde{\rho}_{1c}(t + dt)] \\ &= \zeta [D + (D' - D)\langle n_2 \rangle_c(t)] dt \\ &= \zeta \mathcal{P}_{1c}(t) dt, \end{aligned} \quad (12)$$

where $dN_c(t)$ is a stochastic point process which represents the number (either zero or one) of tunneling events in the QPC seen in an infinitesimal time dt ,

$$\tilde{\rho}_{1c}(t + dt) = \mathcal{J}[T + \chi n_2] \rho_c(t) dt \quad (13)$$

is the unnormalized density matrix [21,22] given the result of an electron tunneling through the QPC barrier at the end of the time interval $[t, t + dt)$, $\langle n_2 \rangle_c(t) = \text{Tr}[n_2 \rho_c(t)]$,

$$\mathcal{P}_{1c}(t) = D + (D' - D)\langle n_2 \rangle_c(t), \quad (14)$$

and $E[Y]$ denotes an ensemble average of a classical stochastic process Y . The subscript c indicates that the quantity to which it is attached is conditioned on previous observations of the occurrences (detection records) of the electrons tunneling through the QPC barrier in the infinitesimal time dt in the past. The factor $\zeta \leq 1$ represents the fraction of tunneling events which are actually registered by the circuit containing the QPC detector. The value $\zeta = 1$ then corresponds to a perfect detector or efficient measurement. By using the fact that current through the QPC is $I(t) = e dN(t)/dt$, Eq. (12) with $\zeta = 1$ states that the average current is eD when the dot is empty, and is eD' when the dot is occupied.

Similarly, we can specify the quantum-jump conditional dynamics through the QD system by defining two stochastic point processes $dM_{Lc}(t)$ and $dM_{Rc}(t)$ which represent, respectively, the numbers (either zeros or ones) of tunneling events from the left lead to dot i and from dot j to the right lead seen in an infinitesimal time dt [21–24]:

$$[dM_{Lc}(t)]^2 = dM_{Lc}(t), \quad [dM_{Rc}(t)]^2 = dM_{Rc}(t), \quad (15)$$

$$E[dM_{Lc}(t)] = \gamma_L \langle c_i^\dagger c_i \rangle_c(t) dt = \gamma_L [1 - \langle n_i \rangle_c(t)] dt, \quad (16)$$

$$E[dM_{Rc}(t)] = \gamma_R \langle c_j^\dagger c_j \rangle_c(t) dt = \gamma_R \langle n_j \rangle_c(t) dt, \quad (17)$$

where $\langle n_j \rangle_c(t) = \text{Tr}[c_j^\dagger c_j \rho_c(t)]$.

Unraveling both the QPC and the QD equations, we write the conditional master equation at zero temperature as

$$\begin{aligned} d\rho_c(t) &= dM_{Lc} \left[\frac{\mathcal{J}[c^\dagger]}{1 - \langle n_i \rangle_c(t)} - 1 \right] \rho_c(t) \\ &\quad + dM_{Rc} \left[\frac{\mathcal{J}[c]}{\langle n_j \rangle_c(t)} - 1 \right] \rho_c(t) \\ &\quad - dt \{ \gamma_L \mathcal{A}[c_i^\dagger] \rho_c(t) + \gamma_R \mathcal{A}[c_j] \rho_c(t) \\ &\quad - \gamma_L [1 - \langle n_i \rangle_c(t)] \rho_c(t) - \gamma_R \langle n_j \rangle_c(t) \rho_c(t) \} \\ &\quad + dN_c \left[\frac{\mathcal{J}[T + \chi n_2]}{\mathcal{P}_{1c}(t)} - 1 \right] \rho_c(t) \\ &\quad + dt \{ -(i/\hbar) [H_S, \rho_c(t)] - \mathcal{A}[T + \chi n] \rho_c(t) \\ &\quad + (1 - \zeta) \mathcal{J}[T + \chi n] \rho_c(t) + \zeta \mathcal{P}_{1c}(t) \rho_c(t) \}. \end{aligned} \quad (18)$$

We now focus on the conditional dynamics of the QD as the QPC current $I(t)$ is continuously monitored. In the experiment, the observed values of the random telegraph process are not fixed at the average values D, D' , but are themselves stochastic processes as electrons tunnel through the QPC. We average over the jump process onto and off the QD. The stochastic quantum-jump master equation of the density matrix operator, conditioned on the observed event in QPC current in the case of inefficient measurement in time dt , can be obtained as

$$\begin{aligned} d\rho_c(t) &= dN_c(t) \left[\frac{\mathcal{J}[T + \chi n]}{\mathcal{P}_{1c}(t)} - 1 \right] \rho_c(t) \\ &\quad + dt \{ -(i/\hbar) [H_S, \rho_c(t)] - \mathcal{A}[T + \chi n] \rho_c(t) \\ &\quad + (1 - \zeta) \mathcal{J}[T + \chi n] \rho_c(t) + \zeta \mathcal{P}_{1c}(t) \rho_c(t) \\ &\quad + \gamma_L \mathcal{D}[c_i^\dagger] \rho_c(t) + \gamma_R \mathcal{D}[c_j] \rho_c(t) \}. \end{aligned} \quad (19)$$

In the quantum-jump case, in which individual electron QPC tunneling current events can be distinguished, the QD system state [see Eq. (19)] undergoes a finite evolution (a *quantum jump*) when there is a detection result [$dN_c(t) = 1$] at randomly determined times (conditionally Poisson distributed).

As Fig. 1(c) of Ref. [25] suggests, the current through the QPC could be quite large and while we may be able to resolve the random telegraph signal jumps between the two average values D and D' , we may not have sufficient bandwidth in the circuit to resolve the jump events $dN(t)$ through the QPC. The individual tunnel events through the QPC are too rapid to be resolved in the external circuit, resulting in a process more like a white-noise stochastic process. This leads us to make the diffusive approximation to the quantum-jump stochastic master equation for describing the conditional QPC current dynamics. We now replace the quantum-jump master equation for the QPC with the quantum diffusion stochastic master equation. In this case, the total number of electrons that tunnel through the QPC in a time δt , large compared to the inverse of the jump rate, but small compared to the typical circuit response time, is considered as a continuous diffusive variable satisfying a Gaussian white-noise distribution [21,22]:

$$\delta N(t) = \{ \zeta |T|^2 [1 + 2\epsilon \cos \theta \langle n_2 \rangle_c(t)] + \sqrt{\zeta} |T| \xi(t) \} \delta t, \quad (20)$$

where $\epsilon = (|\mathcal{X}|/|T|) \ll 1$, θ is the relative phase between \mathcal{X} and T , and $\xi(t)$ is a Gaussian white noise characterized by

$$E[\xi(t)] = 0, \quad E[\xi(t)\xi(t')] = \delta(t - t'). \quad (21)$$

Here, E denotes an ensemble average. In stochastic calculus, $\xi(t)dt = dW(t)$ is known as the infinitesimal Wiener increment. In obtaining Eq. (20), we have assumed that $2|T||\mathcal{X}| \cos \theta \gg |\mathcal{X}|^2$. Hence, for the quantum-diffusive equations obtained later, we should regard, to the order of magnitude, that $|\cos \theta| \sim O(1) \gg \epsilon = (|\mathcal{X}|/|T|)$ and $|\sin \theta| \sim O(\epsilon) \ll 1$.

By taking the diffusive limit on the QPC, the quantum-diffusive conditional master equation for the case of inefficient

measurements can be found as

$$\begin{aligned} \dot{\rho}_c(t) = & -\frac{i}{\hbar}[H_S, \rho_c(t)] \\ & + \gamma_L \mathcal{D}[c_1^\dagger] \rho_c(t) + \gamma_R \mathcal{D}[c_j] \rho_c(t) + \mathcal{D}[T + \chi n_2] \rho_c(t) \\ & + \xi(t) \frac{\sqrt{\zeta}}{|T|} [T^* \chi n_2 \rho_c(t) + \chi^* T \rho_c(t) n_2 \\ & - 2 \operatorname{Re}(T^* \chi) \langle n_2 \rangle_c(t) \rho_c(t)]. \end{aligned} \quad (22)$$

We will now make the simplifying assumption that $\theta = 0$. In that case, T and χ are real and $D = |T|^2$, $D' = |T + \chi|^2$. This corresponds to $D' > D$ as in the experiment of Ref. [25]. The conditional current through the QPC, $I_c(t) = e \delta N(t) / \delta t$, conditioned on the dot occupation, satisfies the stochastic differential equation

$$I_c(t) = e \zeta D [1 - 2\epsilon \langle n_2 \rangle_c(t)] + e \sqrt{\zeta D} \xi(t) \quad (23)$$

with

$$\epsilon = 1 - \sqrt{\frac{D'}{D}}. \quad (24)$$

We can now find from Eq. (22) the conditional dynamics of the dot occupation conditioned on the observed instantaneous QPC current in time dt . For the SQD-QPC system, we have

$$\begin{aligned} \frac{d\langle n_2 \rangle_c(t)}{dt} = & \gamma_L [1 - \langle n_2 \rangle_c(t)] - \gamma_R \langle n_2 \rangle_c(t) \\ & - 2\chi \sqrt{\zeta} [1 - \langle n_2 \rangle_c(t)] \langle n_2 \rangle_c(t) \xi(t). \end{aligned} \quad (25)$$

Note that the noise “turns off” when the dot (dot 2) is either occupied or empty. This can be understood if we regard the QPC current as a measurement of the dot occupation. Suppose that $\gamma_L \neq 0$, and $\gamma_R = 0$, in which case an electron will eventually tunnel onto the dot. The QPC current must eventually reveal this fact, as the current through the QPC will increase. After a small interval of time, we will be confident that this is a real effect and not a random fluctuation and the conditional mean $\langle n_2 \rangle_c$ becomes locked on unity with no further fluctuation. A parallel argument can be made in the case that $\gamma_L = 0$, $\gamma_R \neq 0$. We thus see that this feature of the noise is a reflection of the fact that monitoring the QPC current gives us information on the state of the QD.

Similarly, we obtain from Eq. (22) the equations of motion to determine the DQD coherence and occupations conditioned on the observed instantaneous QPC current in time dt as

$$\begin{aligned} \frac{d\langle n_1 \rangle_c}{dt} = & \gamma_L (1 - \langle n_1 \rangle_c) - i \Omega (\langle c_2^\dagger c_1 \rangle_c - \langle c_1^\dagger c_2 \rangle_c) \\ & + 2\chi \sqrt{\zeta} \xi(t) (\langle n_1 n_2 \rangle_c - \langle n_1 \rangle_c \langle n_2 \rangle_c), \end{aligned} \quad (26)$$

$$\begin{aligned} \frac{d\langle n_2 \rangle_c}{dt} = & -\gamma_R \langle n_2 \rangle_c - i \Omega (\langle c_1^\dagger c_2 \rangle_c - \langle c_2^\dagger c_1 \rangle_c) \\ & + 2\chi \sqrt{\zeta} \xi(t) (\langle n_2 \rangle_c - \langle n_2 \rangle_c^2), \end{aligned} \quad (27)$$

$$\begin{aligned} \frac{d\langle c_1^\dagger c_2 \rangle_c}{dt} = & -\frac{\gamma_L + \gamma_R + \chi^2}{2} \langle c_1^\dagger c_2 \rangle_c + i \Omega (\langle n_2 \rangle_c - \langle n_1 \rangle_c) \\ & + 2\chi \sqrt{\zeta} \xi(t) \left(\frac{1}{2} - \langle n_2 \rangle_c \right) \langle c_1^\dagger c_2 \rangle_c, \end{aligned} \quad (28)$$

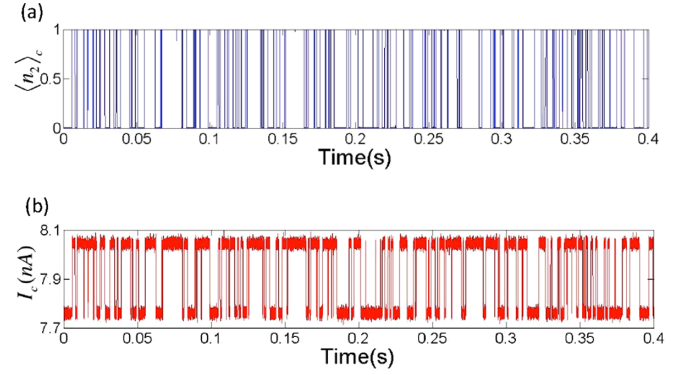


FIG. 2. Simulation of (a) the conditional expectation value of the electron occupation number $\langle n_2 \rangle_c$ and (b) the QPC current. The QPC current is taken with bandwidth of 100 kHz and through a Butterworth filter with eight order and cutoff frequency 4 kHz as in the experiment of Ref. [25] with parameters $(D, D', \gamma_L, \gamma_R) = (4.85 \times 10^{10}, 5.03 \times 10^{10}, 160, 586)$ Hz.

$$\begin{aligned} \frac{d\langle c_2^\dagger c_1 \rangle_c}{dt} = & -\frac{\gamma_L + \gamma_R + \chi^2}{2} \langle c_2^\dagger c_1 \rangle_c + i \Omega (\langle n_1 \rangle_c - \langle n_2 \rangle_c) \\ & + 2\chi \sqrt{\zeta} \xi(t) \left(\frac{1}{2} - \langle n_2 \rangle_c \right) \langle c_2^\dagger c_1 \rangle_c, \end{aligned} \quad (29)$$

$$\begin{aligned} \frac{d\langle n_1 n_2 \rangle_c}{dt} = & -(\gamma_L + \gamma_R) \langle n_1 n_2 \rangle_c + \gamma_L \langle n_2 \rangle_c \\ & + 2\chi \sqrt{\zeta} \xi(t) (1 - \langle n_2 \rangle_c) \langle n_1 n_2 \rangle_c. \end{aligned} \quad (30)$$

It is understood that all the conditional quantum average quantities in Eqs. (26)–(30) carry time dependence, i.e., $\langle \dots \rangle_c \equiv \langle \dots \rangle_c(t)$.

The quantum trajectory theory provides us with full information of the statistical properties about the measured system as that of an experimentalist who actually performs a time-resolved transport experiment. One can use Eq. (25) for the SQD system and Eqs. (26)–(30) for the DQD system to calculate the conditional charge occupation number $\langle n_2 \rangle_c(t)$ and then use Eq. (23) to mimic the measured QPC current record $I_c(t)$ continuously in time in a single run of a realistic experiment. We show in Fig. 2(a) a typical realization of the trajectories of $\langle n_2 \rangle_c(t)$ for the SQD-QPC system obtained by the quantum trajectory theory and in Fig. 2(b) its corresponding conditional QPC current $I_c(t)$ taking into account the detection bandwidth in experiment [25]. The simulated QPC current shows random switchings between two average currents, which correspond to the single-electron tunneling onto and off the QD. It indeed resembles the typical measured QPC current shown in Fig. 1(c) of Ref. [25]. Simulating a great amount of trajectories by many different random realizations of $\xi(t)$, one is able to calculate all the statistical transport quantities of the QD systems, such as the conditional counting statistics. One can obtain the time-average QPC current I in time t by integrating the instantaneous QPC current $I_c(t)$ and acquire the average QD current J conditional on QPC current I in time t in its corresponding $\langle n_2 \rangle_c(t)$ trajectory (see Sec. VII B for details). We simulate a great amount of trajectories and sort J by different I , and use the formulas of the conditional

moments and cumulants to obtain the conditional counting statistics from the data collected from these trajectories.

It is easy to see that the ensemble-average evolution of the conditional master equation (22) reproduces the unconditional master equation (7) by simply eliminating the white-noise term using Eq. (21). Similarly, averaging Eq. (19) over the observed stochastic process, by setting $E[dN_c(t)]$ equal to its expected value (12), gives the unconditional, deterministic master equation (7). It is also easy to verify that for zero efficiency $\zeta = 0$ [i.e., also $dN_c(t) = 0$], the conditional equations (19) and (22) reduce to the unconditional one, (7). That is, the effect of averaging over all possible measurement records is equivalent to the effect of completely ignoring the detection records or the effect of no detection results being available.

V. NUMBER-RESOLVED MASTER EQUATION

To study the current cumulants of one conductor (e.g., the QD system) conditioned on the average current of the other conductor (e.g., the QPC), we turn to the number-resolved master equation [15,20,32,33] or the master equation for the partially reduced density matrix [23,24] of the joint QD and QPC system. If N electrons have tunneled through the QPC and M electrons have tunneled through the right junction of the QD at time $t + dt$, then the accumulated number of electrons in the drain of the QPC at the earlier time t , due to the contribution of the *jump* term of the QPC, should be $(N - 1)$ for M electron in the drain of the QD, and it should be $(M - 1)$ in the drain (right lead) of the QD system due to the contribution of the *jump* term of the QD for N electron in the drain of the QPC [23,24]. Hence, after writing out the number dependence N , $(N - 1)$, M , or $M - 1$ explicitly for the density matrix in Eq. (7), we obtain the master equation for the “partially” reduced density matrix as

$$\begin{aligned} \dot{\rho}(N, M, t) = & -(i/\hbar)[H_S, \rho_c(N, M, t)] \\ & + \zeta \mathcal{J}[T + \mathcal{X}n]\rho(N - 1, M, t) \\ & + (1 - \zeta)\mathcal{J}[T + \mathcal{X}n]\rho(N, M, t) \\ & - \mathcal{A}[T + \mathcal{X}n]\rho(N, M, t) \\ & + \gamma_L \mathcal{D}[c_i^\dagger]\rho(N, M, t) - \gamma_R \mathcal{A}[c_j]\rho(N, M, t) \\ & + \gamma_R \mathcal{J}[c_j]\rho(N, M - 1, t). \end{aligned} \quad (31)$$

If the sum over all possible values of N and M is taken on the “partially” reduced density matrix [i.e., $\rho(t) = \sum_{N, M} \rho(N, M, t)$], Eq. (31) then reduces to Eq. (7).

For simplicity, in the following we set the QPC detection efficiency $\zeta = 1$ corresponding to perfect detections or efficient measurements. We deal with the case of the SQD-QPC system first. After evaluating Eq. (31) in the occupation number basis $|0\rangle$ and $|1\rangle$ of the SQD, we obtain the rate equations as

$$\begin{aligned} \dot{\rho}_{00}(N, M, t) = & |T|^2 \rho_{00}(N - 1, M, t) - |T|^2 \rho_{00}(N, M, t) \\ & - \gamma_L \rho_{00}(N, M, t) + \gamma_R \rho_{11}(N, M - 1, t), \quad (32) \\ \dot{\rho}_{11}(N, M, t) = & |T + \mathcal{X}|^2 \rho_{11}(N - 1, M, t) \\ & - |T + \mathcal{X}|^2 \rho_{11}(N, M, t) \\ & + \gamma_L \rho_{00}(N, M, t) - \gamma_R \rho_{11}(N, M, t), \quad (33) \end{aligned}$$

where $\rho_{aa} = \langle a | \rho | a \rangle$ with $a = 0, 1$ referring to the QD occupation number states.

To obtain the solution of $\rho_{aa}(N, M, t)$ with $a = 0, 1$ in the number-resolved or the “partially” reduced density matrix approach, we can first apply a two-dimensional Fourier transform (to the counting field space) [23,24,32,33]

$$\rho_{aa}(k, q, t) = \sum_{N, M} e^{ikN + iqM} \rho_{aa}(N, M, t) \quad (34)$$

to Eqs. (32) and (33) since these equations are translationally invariant in N and M space. So, after the Fourier transform, we obtain from Eqs. (32) and (33) that

$$\frac{d\rho(k, q, t)}{dt} = \mathcal{L}(k, q)\rho(k, q, t), \quad (35)$$

where

$$\begin{aligned} \rho(k, q, t) = & \begin{pmatrix} \rho_{00}(k, q, t) \\ \rho_{11}(k, q, t) \end{pmatrix}, \quad (36) \\ \mathcal{L}(k, q) = & \begin{pmatrix} D(e^{ik} - 1) - \gamma_L & \gamma_R e^{iq} \\ \gamma_L & D'(e^{ik} - 1) - \gamma_R \end{pmatrix}. \quad (37) \end{aligned}$$

We note here again that we have set T and \mathcal{X} to be real and their relative phase angle $\theta = 0$ so that $D = |T|^2$, $D' = |T + \mathcal{X}|^2$.

Similarly for the case of coherently coupled DQD's measured by a QPC [see Fig. 1(b)], the number-resolved master equation in the Fourier space (counting field space) can also be written in the form of Eq. (35) with $\mathcal{L}(k, q)$ given in matrix form as

$$\mathcal{L}(k, q) = \begin{pmatrix} f(k) - \gamma_L & 0 & \gamma_R e^{iq} & 0 & 0 & 0 \\ \gamma_L & f(k) & 0 & \gamma_R e^{iq} & 0 & 2\Omega \\ 0 & 0 & f'(k) - 2\gamma & 0 & 0 & -2\Omega \\ 0 & 0 & \gamma_L & f'(k) - \gamma_R & 0 & 0 \\ 0 & 0 & 0 & 0 & g(k) & -\Delta\epsilon \\ 0 & -\Omega & \Omega & 0 & \Delta\epsilon & g(k) \end{pmatrix}, \quad (38)$$

and the column vector density matrix defined as $\rho^T = (\rho_{00}, \rho_{LL}, \rho_{RR}, \rho_{11}, \text{Re}\rho_{LR}, \text{Im}\rho_{LR})$. Here, the matrix elements $\rho_{ab} = \rho_{ab}(k, q, t)$, with indices $a, b \in \{0, L, R, 1\}$, denote the

Fock states $|00\rangle$, $|10\rangle$, $|01\rangle$, and $|11\rangle$ of the system, i.e., no electron, one electron in the first dot (left dot), one electron in the second dot (right dot), and one in each

dot, respectively. The functions $f(k) = D(e^{ik} - 1)$, $f'(k) = D'(e^{ik} - 1)$, and $g(k) = \sqrt{DD'}e^{ik} - D_a - \Gamma$, where $D = |T|^2$, $D' = |T + \chi|^2$, $\Gamma = (\gamma_L + \gamma_R)/2$, $D_0 = (D + D')/2$, $\Delta\epsilon = \epsilon_2 - \epsilon_1$.

The factor

$$\Gamma_d = \frac{(\sqrt{D'} - \sqrt{D})^2}{2} = \frac{|\chi|^2}{2} \quad (39)$$

appears in the diagonal elements of the last two rows of the resultant matrix $\mathcal{L}(k=0, q=0)$ of Eq. (38) and thus plays the role of dephasing rate for the unconditional dynamics of the DQD's. As Γ_d becomes larger, the QPC tends to localize the electron on the dot and thus reduces the coherent tunneling

Ω that changes the DQD states between $|01\rangle$ and $|10\rangle$. When $\Omega \ll \Gamma_d$, one expects $\text{Re}\rho_{LR}$ and $\text{Im}\rho_{LR}$ from the last two rows of the master equation (35) with $\mathcal{L}(k=0, q=0)\rho$ defined in Eq. (38) will decay much faster than other density matrix elements. As a result, one can set the last two rows of Eq. (38) equal to zero and then substitute the solution of $\text{Re}\rho_{LR}$ and $\text{Im}\rho_{LR}$ back to the coupled equation. Thus, we obtain an effective tunneling rate between the two dots as

$$\Gamma_\Omega = \frac{2\Omega^2/(\Gamma + \Gamma_d)}{[1 + (\frac{\Delta\epsilon}{\Gamma})^2]}. \quad (40)$$

In this case, the 6×6 coherent tunneling matrix of $\mathcal{L}(k, q)$ in the master equation in the Fourier space (counting field space) reduces to a 4×4 sequential tunneling matrix

$$\mathcal{L}_{\text{seq}}(k, q) = \begin{pmatrix} f(k) - \gamma_L & 0 & \gamma_R e^{iq} & 0 \\ \gamma_L & f(k) - \Gamma_\Omega & \Gamma_\Omega & \gamma_R e^{iq} \\ 0 & \Gamma_\Omega & f'(k) - 2\gamma - \Gamma_\Omega & 0 \\ 0 & 0 & \gamma_L & f'(k) - \gamma_R \end{pmatrix} \quad (41)$$

with Γ_d defined in Eq. (39), and the column vector density matrix becomes $\rho^T = (\rho_{00}, \rho_{LL}, \rho_{RR}, \rho_{11})$ involved only the population elements.

In principle, one can solve the resultant coupled first-order differential equations obtained from Eq. (35) for the column elements of $\rho_{ab}(k, q, t)$ and then perform an inverse Fourier transform to obtain $\rho_{ab}(N, M, t)$. The probability distribution of finding N electrons that have tunneled through the QPC and M electrons that have tunneled into the drain of the QD during time t can then be obtained as

$$\begin{aligned} P(N, M, t) &= \text{Tr}_{\text{dot}}[\rho(N, M, t)] \\ &= \sum_a \rho_{aa}(N, M, t) \\ &= \int_0^{2\pi} \int_0^{2\pi} \frac{dk dq}{(2\pi)^2} e^{-ikN - iqM} \sum_a \rho_{aa}(k, q, t). \end{aligned} \quad (42)$$

From this distribution function $P(N, M, t)$, all orders of unconditional and conditional cumulants (counting statistics) of transmitted electrons can be in principle calculated.

VI. COUNTING STATISTICS: GENERATING FUNCTIONAL APPROACH

A. Unconditional counting statistics

In practice, a more efficient method is the generating functional technique. One may define the moment generating function as [14]

$$e^{-F(k, q, t)} = \sum_{N, M} P(N, M, t) e^{ikN + iqM}. \quad (43)$$

From this definition, it is easy to check that the n th moment of N and the m th moment of M can be written as

$$\langle N^n M^m \rangle(t) = (-i\partial_k)^n (-i\partial_q)^m e^{-F(k, q, t)}|_{k=0=q}. \quad (44)$$

The cross cumulants can be calculated through the cumulant generating function $F(k, q, t)$ as

$$\langle\langle N^n M^m \rangle\rangle(t) = -(-i\partial_k)^n (-i\partial_q)^m F(k, q, t)|_{k=0=q}. \quad (45)$$

For example, $\langle\langle O \rangle\rangle = \langle O \rangle$, $\langle\langle O^2 \rangle\rangle = \langle (O - \langle O \rangle)^2 \rangle$, $\langle\langle O^3 \rangle\rangle = \langle (O - \langle O \rangle)^3 \rangle$, $\langle\langle O^4 \rangle\rangle = \langle (O - \langle O \rangle)^4 \rangle - 3\langle (O - \langle O \rangle)^2 \rangle^2$, etc.

From Eqs. (43), (42), and (34), the moment generating function can then be obtained from $\rho(k, q, t)$ as

$$e^{-F(k, q, t)} = \text{Tr}_{\text{dot}}[\rho(k, q, t)] = \sum_a \rho_{aa}(k, q, t), \quad (46)$$

and the cumulant generating function is then

$$F(k, q, t) = -\ln \left[\sum_a \rho_{aa}(k, q, t) \right]. \quad (47)$$

As a result, the unconditional moments and cumulants can be calculated using Eqs. (46) and (47) according to Eqs. (44) and (45).

Thus, the solution of the number-resolved master equation in the Fourier space (counting field space) $\rho(k, q, t)$ has a direct connection with the generating function approach to calculate the FCS.

B. Conditional counting statistics

Having described the joint statistical properties of both the QPC and QD currents, we discuss the conditional counting statistics: the statistical current fluctuations (cumulants) of one system given the observation of a given average current in the other system in time t .

In QD-QPC transport system, the probability of having M electrons tunneling into the drain of the QD system conditioned on N electrons passing through QPC in time t can be written as

$$P(M|N, t) = P(N, M, t)/P(N, t). \quad (48)$$

By defining the conditional moment generating function as

$$e^{F_c(N,q,t)} \equiv \sum_M P(M|N,t) e^{iqM}, \quad (49)$$

the r th moment of electron number M passing through the QD system, conditioned on the number of electrons N in the drain of the QPC, is given by

$$\langle M^r(t) \rangle_c = \sum_M M^r P(M|N,t) = \partial_{iq}^r e^{F_c(N,q,t)}|_{q=0}, \quad (50)$$

where the subscript “ c ” denotes the quantity it attaches to being conditional. The conditional cumulant $\langle\langle M^r(t) \rangle\rangle_c$ could be found by taking partial derivatives with respect to (iq) on the conditional cumulant generating function $F_c(N,q,t)$:

$$\langle\langle M^r(t) \rangle\rangle_c = \partial_{iq}^r F_c(N,q,t)|_{q=0}. \quad (51)$$

Using Eqs. (48) and (49), one observes that the conditional cumulant generating function which is the logarithm of the conditional moment generating function can be effectively rewritten as

$$F_c(N,q,t) = -\ln P(N,q,t), \quad (52)$$

where

$$\begin{aligned} P(N,q,t) &= \sum_M P(N,M,t) e^{iqM} \\ &= \frac{1}{2\pi} \int_0^{2\pi} dk P(k,q,t) e^{-ikN}. \end{aligned} \quad (53)$$

In obtaining Eq. (53), we have used the fact that $P(N,q,t)$ can also be expressed as the inverse Fourier transform of $P(k,q,t)$ with respect to the counting field variable k . Since $P(k,q,t) = \text{Tr}_{\text{dot}}[\rho(k,q,t)] = \sum_a \rho_{aa}(k,q,t)$, one can calculate the conditional counting statistics once having the solution of the number-resolved master equation in the Fourier space (counting field space) $\rho(k,q,t)$.

C. FCS in the stationary state

Unconditional current cumulant. In the stationary or steady state ($t \rightarrow \infty$), the calculation of moments or cumulants can be simplified. The solution of Eq. (35) can be symbolically written as

$$\rho(k,q,t) = e^{\mathcal{L}(k,q)t} \rho(k,q,0). \quad (54)$$

There is a unique eigenvalue $\lambda_1(k,q)$ of $\mathcal{L}(k,q)$ which develops from the zero eigenvalue of $\mathcal{L}(k=0, q=0)$ with the smallest absolute real part. The rest of the eigenvalue(s) has (have) larger finite negative real parts that make their contributions considerably much smaller for large times. As a consequence, the long-time dynamics of the moment generating functional (46) near the stationary state can be well approximated as [14,25]

$$e^{-F(k,q,t)} = \text{Tr}_{\text{dot}}[\rho(k,q,t)] \approx e^{\lambda_1(k,q)t}. \quad (55)$$

For the SQD-QPC system, the eigenvalue $\lambda_1(k,q)$ can be found from Eq. (37) to be

$$\begin{aligned} \lambda_1(k,q) &= (e^{ik} - 1)D_0 - \Gamma \\ &\quad + \sqrt{[(e^{ik} - 1)\Delta D - \Delta\Gamma]^2 + \gamma_L\gamma_R e^{iq}}, \end{aligned} \quad (56)$$

where $D_0 = (D + D')/2$, $\Gamma = (\gamma_L + \gamma_R)/2$, $\Delta D = (D - D')/2$, and $\Delta\Gamma = (\gamma_L - \gamma_R)/2$. Similarly, the long-time (stationary-state) probability distribution function from Eqs. (42) and (55) can be approximated as

$$P(N,M,t) = \int_0^{2\pi} \int_0^{2\pi} \frac{dk dq}{(2\pi)^2} e^{-ikN - iqM + \lambda_1(k,q)t}. \quad (57)$$

We can define the QPC current $I = N/t$ and QD current $J = M/t$ (setting $e = 1$) in time t . Replacing $N = It$ and $M = Jt$, we then obtain the distribution function of the two currents

$$P(I,J,t) = \int_0^{2\pi} \int_0^{2\pi} \frac{dk dq}{(2\pi)^2} e^{[\lambda_1(k,q) - ikI - iqJ]t}. \quad (58)$$

In the long-time (stationary) limit where the time t should be much larger than $\gamma_{L,R}^{-1}$, we may thus evaluate the integral (58) in the stationary phase approximation. The dominant contribution to the joint probability distribution then takes the form of a Legendre transform [25]:

$$\ln[P(I,J,t)] = t \min_{k,q} [\lambda_1(k,q) - ikI - iqJ]. \quad (59)$$

Since the long-time charge-number cumulant generating function $F(k,q,t)$ from Eq. (55) is linear in time, we may define the long-time (stationary-state) current cumulant generating function as $\lambda_1(k,q)$, which is time independent. The stationary-state current cumulant can then be calculated through

$$\begin{aligned} \langle\langle I^n J^m \rangle\rangle &= \langle\langle N^n M^m \rangle\rangle / t \\ &= (-i\partial_k)^n (-i\partial_q)^m \lambda_1(k,q)|_{k=0=q}. \end{aligned} \quad (60)$$

Note that the time dependence drops out in the expression of the stationary-state current cumulant of Eq. (60).

For example, the zero-frequency QD current noise and QPC current noise can also be calculated:

$$\begin{aligned} \langle\langle J^2 \rangle\rangle &= (-i\partial_q^2) \lambda_1(k,q)|_{k=q=0} \\ &= \frac{\gamma_L \gamma_R (\gamma_L^2 + \gamma_R^2)}{(\gamma_L + \gamma_R)^3}, \quad (61) \\ \langle\langle I^2 \rangle\rangle &= (-i\partial_k^2) \lambda_1(k,q)|_{k=q=0} \\ &= \frac{2(D - D')^2 \gamma_L \gamma_R}{(\gamma_L + \gamma_R)^3} \\ &\quad + \frac{S(0)_0}{2} \left(\frac{\gamma_R}{\gamma_L + \gamma_R} \right) + \frac{S(0)_1}{2} \left(\frac{\gamma_L}{\gamma_L + \gamma_R} \right), \quad (62) \end{aligned}$$

where $S(0)_0 = 2D$ and $S(0)_1 = 2D'$ are the values of the shot noise of the QPC for the QD (dot 2) in $|0\rangle$ and $|1\rangle$ states, respectively. The first term of the QPC current noise of Eq. (62) comes from the random telegraph process in the QPC currents making transitions between D and D' caused by the electrons randomly tunneling onto and out of dot 2 with rates γ_L and γ_R , respectively.

Conditional current cumulant. Similarly, in the stationary state, the conditional current cumulant generating function $\lambda_{cI}(I,q)$ and $\lambda_{cJ}(J,q)$ can be calculated from the reverse partial Fourier transform of the joint generating

function [25]

$$e^{\lambda_{cI}(I,q)t} = P(I,q,t) = \int_0^{2\pi} \frac{dk}{(2\pi)} e^{[\lambda_1(k,q) - ikI]t}, \quad (63)$$

$$e^{\lambda_{cJ}(k,J)t} = P(k,J,t) = \int_0^{2\pi} \frac{dq}{(2\pi)} e^{[\lambda_1(k,q) - iqJ]t}. \quad (64)$$

One may evaluate the integral in the stationary phase approximation to obtain [25]

$$\lambda_{cI}(I,q) = \min_k [\lambda_1(k,q) - ikI], \quad (65)$$

$$\lambda_{cJ}(k,J) = \min_q [\lambda_1(k,q) - iqJ]. \quad (66)$$

The conditional current cumulant then can be calculated from

$$\langle\langle J^m \rangle\rangle_c = (-i\partial_q)^m \lambda_{cI}(I,q)|_{q=0}, \quad (67)$$

$$\langle\langle I^n \rangle\rangle_c = (-i\partial_k)^n \lambda_{cJ}(k,J)|_{k=0}. \quad (68)$$

However, the conditional current cumulant generating functions of Eqs. (65) and (66) are difficult to evaluate unless an analytic form of the eigenvalue $\lambda_1(k,q)$ is available. Even for the problem of the SQD-QPC system where the eigenvalue $\lambda_1(k,q)$ can be obtained analytically, it is still not easy to evaluate Eqs. (65) and (66) directly. In Ref. [25], a further approximation to neglect the shot-noise contribution from the QPC was made. As a result, the calculations are significantly simplified and the conditional generating functions and conditional current cumulants were obtained in analytical forms. From the zero-frequency noise of Eq. (62), the QPC shot-noise terms (the last two terms) can be neglected as compared to the first term when the parameters $(D - D')^2 \gg (D, D')(\gamma_L + \gamma_R)$. In Ref. [25], the QPC tunneling rates are set to be $D' \approx 5.03 \times 10^{10}$ Hz and $D \approx 4.85 \times 10^{10}$ Hz, and the QD tunneling rates are chosen as $\gamma_L = 160$ Hz, $\gamma_R = 586$ Hz in configuration A and $\gamma_L = 512$ Hz, $\gamma_R = 345$ Hz in configuration B. So, it was valid to neglect the QPC shot-noise terms for the parameters used in Ref. [25]. Neglecting the QPC shot-noise terms amounts to replacing $e^{ik} \rightarrow 1 + ik$ in Eq. (56). Consequently, the conditional current cumulant generating functions of Eqs. (65) and (66) can be obtained analytically, so are the conditional current cumulants. However, when the QPC shot-noise terms cannot be neglected, the conditional steady-state generating functions of Eqs. (65) and (66) and thus also the conditional current cumulants (67) and (68) are difficult to obtain even using the analytic form of the eigenvalue of Eq. (56) due to the fact that the numerical minimization and then numerical derivatives that need to be performed are quite numerically unstable. It is even more difficult for more complicated interacting nanoscale conductors with the dimension of the matrix equation of the master equation growing quickly and no analytical forms of eigenvalues of $\mathcal{L}(k,q)$ are available.

D. Efficient numerical method

It is thus desirable to develop an efficient and numerically stable method to calculate the conditional counting statistics for a wider range of parameters and for more complicated interacting quantum transport systems. For unconditional

steady-state cumulants, the projection operator technique with perturbation expansion in counting fields developed in Refs. [19,35–38] can be used to circumvent the problems of large system dimensions and the instability of taking numerical derivatives on the generating function. However, things are different in the conditional case. The unconditional cumulants are evaluated in the counting field (inverse Fourier transform) space, e.g., the steady-state cross-current cumulant of Eq. (60). Thus, a perturbation partition of the Liouvillian matrix $\mathcal{L}(k,q)$ in Eq. (35) can be performed to calculate corrections to the maximum eigenvalue [with counting fields set to zero, e.g., $\lambda_1(k=0, q=0)$] order by order in the counting fields to avoid taking derivatives. In contrast, the conditional cumulants are evaluated in the partial or mixed Fourier transform space, i.e., the mixed space of counting field of one system and tunneled electron number of the other system, e.g., the conditional current cumulant of Eq. (67) in which $I = N/t$. Thus, even though the perturbation expansion can be performed in the counting field q , the Liouvillian matrix $\mathcal{L}(N,q)$ in the mixed N -resolved and counting field master equation will couple the N -sector density matrix elements with the $(N - 1)$ -sector ones, forming huge coupled difference equations that are difficult to solve. To proceed, one crucial observation is that the conditional moment of Eq. (50), with the help of Eqs. (48), (49), and (53), can be written as

$$\langle M^r(t) \rangle_c = \frac{1}{2\pi P(N,t)} \int_0^{2\pi} dk \text{Tr}_{\text{dot}} [\partial_{iq}^r \rho(k,q,t)|_{q=0}] e^{-ikN}, \quad (69)$$

where $P(N,t) = \frac{1}{2\pi} \int_0^{2\pi} dk \text{Tr}_{\text{dot}} [\rho(k,q,t)|_{q=0}] e^{-ikN}$. Thus, if we can find out how the r th derivatives $\partial_{iq}^r \rho(k,q,t)|_{q=0}$ evolve in time t directly, then we can just perform the trace and inverse Fourier transform to obtain directly the moments of electron number through the QD system conditioned on a given QPC current.

To find the evolution equations for the variables $\partial_{iq}^r \rho(k,q,t)|_{q=0}$, let us take partial derivatives with respect to the counting factor iq on Eq. (35) r times for the QD system and then set $q = 0$. We obtain r differential equations as [34]

$$\begin{aligned} \dot{\rho}(k,q,t)|_{q=0} &= \mathcal{L}(k,q)\rho(k,q,t)|_{q=0}, \\ \partial_{iq} \dot{\rho}(k,q,t)|_{q=0} &= \partial_{iq} [\mathcal{L}(k,q)\rho(k,q,t)]|_{q=0}, \\ \partial_{iq}^2 \dot{\rho}(k,q,t)|_{q=0} &= \partial_{iq}^2 [\mathcal{L}(k,q)\rho(k,q,t)]|_{q=0}, \\ &\vdots \\ \partial_{iq}^r \dot{\rho}(k,q,t)|_{q=0} &= \partial_{iq}^r [\mathcal{L}(k,q)\rho(k,q,t)]|_{q=0}. \end{aligned} \quad (70)$$

Note that with the expression of $\mathcal{L}(k,q)$ available [e.g., given by Eq. (37) or (38)], the derivatives of

$$\begin{aligned} \partial_{iq}^r [\mathcal{L}(k,q)\rho(k,q,t)]|_{q=0} &= \{[\partial_{iq}^r \mathcal{L}(k,q)]\rho(k,q,t)\}|_{q=0} \\ &\quad + \{\mathcal{L}(k,q)[\partial_{iq}^r \rho(k,q,t)]\}|_{q=0} \end{aligned} \quad (71)$$

in Eq. (70) should be evaluated first. Then, the equation resulting from Eq. (70) forms a set of coupled differential equations for variables $\partial_{iq}^r \rho(k,q,t)|_{q=0}$. In this way, the derivatives of $\partial_{iq}^r \rho(k,q,t)|_{q=0}$ can be considered as being performed beforehand as one can obtain the solutions for the r th derivatives $\partial_{iq}^r \rho(k,q,t)|_{q=0}$ directly [34] and can thus avoid taking the derivatives later on the generating functions

(if the generating functions were obtained numerically first), which are often quite numerically unstable. We can define a supervector σ as

$$\sigma(k, q = 0, t) = \begin{pmatrix} \rho(k, q, t)|_{q=0} \\ \partial_{iq} \rho(k, q, t)|_{q=0} \\ \partial_{iq}^2 \rho(k, q, t)|_{q=0} \\ \vdots \\ \partial_{iq}^r \rho(k, q, t)|_{q=0} \end{pmatrix} \quad (72)$$

and write Eq. (70) as

$$\dot{\sigma}(k, q = 0, t) = Z(k, q = 0)\sigma(k, q = 0, t), \quad (73)$$

where the $Z(k, q = 0)$ matrix contains all the elements of \mathcal{L} and its partial derivatives. The solution of Eq. (73) can be obtained by the exponentiation of the $Z(k, q = 0)t$ matrix as

$$\sigma(k, q = 0, t) = e^{Z(k, q=0)t} \sigma(k, q = 0, t = 0). \quad (74)$$

Performing the inverse Fourier transform of the supervector $\sigma(k, q = 0, t)$, then tracing over the system degree of freedom on the r th derivative components of the resultant supervector, and finally divide the quantity by the probability $P(N, t)$, one obtains the conditional moment $\langle M^r \rangle_c$. Note that $P(N, t)$ is just the trace of the 0th derivative components of the resultant inverse-Fourier-transformed supervector over the system degrees of freedom. The conditional current cumulants can be obtained from the conditional moments $\langle M^r \rangle_c$. For example, the first and second conditional current cumulants are obtained by

$$\langle \langle J \rangle \rangle_c = \frac{\langle M \rangle_c}{t}, \quad (75)$$

$$\langle \langle J^2 \rangle \rangle_c = \frac{\langle M^2 \rangle_c - \langle M \rangle_c^2}{t}. \quad (76)$$

This method can be applied to deal with more complex systems with larger dimension of the $Z(k, q)$ matrices.

In summary, to avoid numerical instability and complexity of taking derivatives on the generating functions, we develop an efficient numerical method to calculate the conditional moments and cumulants for more complicated interacting quantum transport systems. This method also allows the calculations of both transient and stationary conditional counting statistics. To demonstrate its advantage and usage, we will apply this method to calculate the first and second current cumulants of two nanoscale interacting conductor systems. The first one is just the SQD-QPC system but without ignoring the QPC shot noise. The second one is a more complicated system of DQD's in series with one of the dots measured by a QPC, for which analytical eigenvalues of matrix $\mathcal{L}(k, q)$ of the evolution equation for general parameters are not available.

Considering, for example, the QPC shot noise without replacing $e^{ik} \rightarrow 1 + ik$ for the SQD-QPC system, we can write in our numerical method the matrix form $\dot{\sigma}(k, q, t) = Z(k, q)\sigma(k, q, t)$ to calculate the first and second QD current moments and cumulants conditioned on the QPC current I ,

where

$$\sigma(k, q, t) = \begin{pmatrix} \rho_{00}(k, q, t) \\ \rho_{11}(k, q, t) \\ \partial_{iq} \rho_{00}(k, q, t) \\ \partial_{iq} \rho_{11}(k, q, t) \\ \partial_{iq}^2 \rho_{00}(k, q, t) \\ \partial_{iq}^2 \rho_{11}(k, q, t) \end{pmatrix} \quad (77)$$

and

$$Z(k, q) = \begin{pmatrix} f_1(k) & \gamma_R e^{iq} & 0 & 0 & 0 & 0 \\ \gamma_L & f_2(k) & 0 & 0 & 0 & 0 \\ 0 & \gamma_R e^{iq} & f_1(k) & \gamma_R e^{iq} & 0 & 0 \\ 0 & 0 & \gamma_L & f_2(k) & 0 & 0 \\ 0 & \gamma_R e^{iq} & 0 & 2\gamma_R e^{iq} & f_1(k) & \gamma_R e^{iq} \\ 0 & 0 & 0 & 0 & \gamma_L & f_2(k) \end{pmatrix}, \quad (78)$$

with $f_1(k) = D(e^{ik} - 1) - \gamma_L$ and $f_2(k) = D'(e^{ik} - 1) - \gamma_R$.

VII. RESULT AND DISCUSSION

We focus on the first two orders of the QD current cumulants, i.e., $\langle \langle J \rangle \rangle_c$ and $\langle \langle J^2 \rangle \rangle_c$, conditioned on an observed QPC current I . We will vary the QPC tunneling rates such that the difference in the QPC tunneling rates with and without the occupation of an electron on dot 2 goes from high to low, and at the same time the condition to ignore the QPC shot noise term is also progressively not satisfied. We will take the QD tunneling rates to be $\gamma_L = 160$ Hz, $\gamma_R = 586$ Hz which are the same as those of configuration A in Ref. [25]. As stated earlier, the QPC shot-noise terms of the second and third terms of Eq. (62) can be neglected as compared to the first term of the random-telegraph-process noise when $(D' - D)^2 \gg (D, D')(\gamma_L + \gamma_R)$. Since the values of $(D', D) = (5.03 \times 10^{10}, 4.85 \times 10^{10})$ Hz have already been demonstrated in Ref. [25] to be an excellent parameter set to neglect the QPC shot noise, we specifically choose three sets of the QPC tunneling rates to be $(D', D) = (5.03 \times 10^8, 4.85 \times 10^8)$ Hz, $(5.03 \times 10^7, 4.85 \times 10^7)$ Hz, $(5.03 \times 10^6, 4.85 \times 10^6)$ Hz to investigate the effect of shot noise. Note that these values of (D, D') in front of the exponents in the three sets of (D, D') are the same. As a result, when the QPC tunneling rate (i.e., the exponent) decreases, the random telegraph signal will no longer dominate over the QPC shot-noise contribution and therefore the QPC shot noise cannot be neglected completely. In other words, the analytic method that replaces $e^{ik} \rightarrow 1 + ik$ in Ref. [25] will be progressively not valid as the QPC tunneling rates in the three sets of (D, D') decrease from high to low.

A. SQD-QPC system

We will show how the QPC shot noise (intrinsic noise) affects the conditional current cumulants for the SQD-QPC system through the quantities of the joint probability distribution $P(I, J, t)$ of detecting the QPC current I and QD current J , and the conditional current $\langle \langle J \rangle \rangle_c$ and conditional zero-frequency noise $\langle \langle J^2 \rangle \rangle_c$.

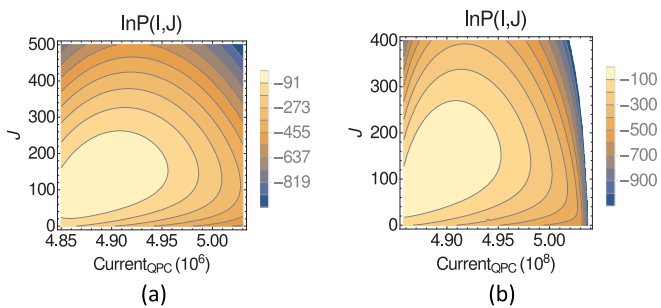


FIG. 3. The logarithm of the joint probability distribution, $\ln P(I, J)$, of observing SQD current J and QPC current I as a color contour plot obtained by using maximum eigenvalue method for (a) $(D', D) = (5.03 \times 10^6, 4.85 \times 10^6)$ Hz, (b) $(D', D) = (5.03 \times 10^8, 4.85 \times 10^8)$ Hz. The tunneling rates of the SQD are $\gamma_L = 160$ Hz and $\gamma_R = 586$ Hz.

1. Joint probability distribution

With the maximum eigenvalue $\lambda_1(k, q)$ of Eq. (56) available, it is possible to obtain the joint probability distribution $P(I, J)$ from Eq. (59) without replacing $e^{ik} \rightarrow 1 + ik$. The contour plots of the logarithm of the joint probability distribution $\ln P(I, J)$ of detecting QPC current I (horizontal axis) and QD current J (vertical axis) for $(D', D) = (5.03 \times 10^6, 4.85 \times 10^6)$ Hz and $(D', D) = (5.03 \times 10^8, 4.85 \times 10^8)$ Hz are shown in Figs. 3(a) and 3(b), respectively. The logarithm of the joint probability distribution in Fig. 3(a), with low QPC tunneling rates (D, D') for which $(D' - D)^2$ is comparable to $(D, D')(\gamma_L + \gamma_R)$, differs considerably from that of neglecting the QPC current shot noise presented in Ref. [25]. Especially near the end points of $I = D$ and D' , substantially larger probabilities for finite J values are observed here. This indicates (see the discussion in the next paragraph about the conditional current probability) that the resultant conditional QD current and noise conditioned on the observed QPC current at or near $I = D$ and D' will deviate from zeros as those shown in Ref. [25]. For the parameter set of higher QPC tunneling rates shown in Fig. 3(b), the the logarithm of joint current probability distribution looks closer to that of Ref. [25].

The conditional QD current probability $P(J|I, t)$ can be obtained from the joint current probability distribution $P(I, J, t)$ using the Bayesian formalism as

$$P(J|I, t) = \frac{P(I, J, t)}{P(I, t)} = \frac{P(I, J, t)}{\int dJ P(I, J, t)}. \quad (79)$$

With conditional current probability, we can calculate the conditional quantities. The conditional current moments can be obtained directly from $P(J|I, t)$ as $\langle J^r(t) \rangle_c \equiv \int_0^\infty dJ P(J|I, t) J^r(t)$ and the conditional current cumulants $\langle\langle J^r(t) \rangle\rangle_c$ can be calculated from $\langle J^r(t) \rangle_c$ accordingly, e.g., $\langle\langle J^2 \rangle\rangle_c = \langle J^2 \rangle_c - \langle J \rangle_c^2$. We will show in the next section the results of the conditional QD current and zero-frequency noise (the first and second conditional cumulants) using the method of the joint current probability distribution and the Bayesian formalism as a confirmation of our numerical method for the SQD-QPC case.

Integrating the conditional $\langle J^r(t) \rangle_c$ over the QPC current probability $P(I, t)$ gives the corresponding unconditional cur-

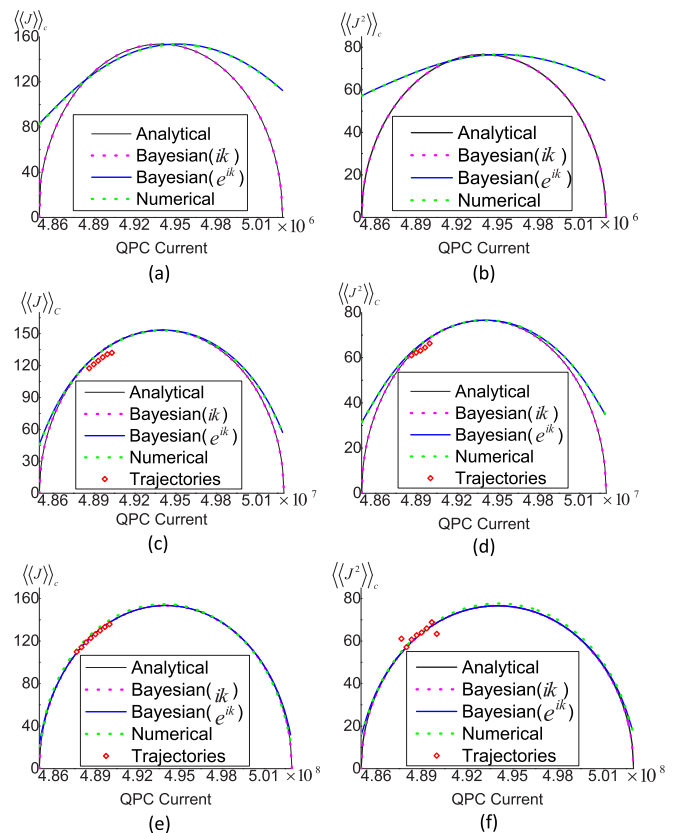


FIG. 4. Conditional SQD current, the first cumulant (left panel) and zero-frequency noise, the second cumulant (right panel) obtained by different methods for (a) and (b) $(D', D) = (5.03 \times 10^6, 4.85 \times 10^6)$ Hz, (c) and (d) $(D', D) = (5.03 \times 10^7, 4.85 \times 10^7)$ Hz, and (e) and (f) $(D', D) = (5.03 \times 10^8, 4.85 \times 10^8)$ Hz. The tunneling rates of the SQD are $(\gamma_L, \gamma_R) = (160, 586)$ Hz.

rent moments: $\langle J^r(t) \rangle = \int_0^\infty dI P(I, t) \langle J^r(t) \rangle_c$. This formula demonstrates that the conditional quantities $\langle J^r(t) \rangle_c$ provides us with more information and can give insight into the unconditional quantities.

2. First and second conditional current cumulants

The first and second steady-state conditional QD current cumulants $\langle\langle J \rangle\rangle_c$ and $\langle\langle J^2 \rangle\rangle_c$ shown in Figs. 4(a) and 4(b) for low QPC tunneling rates $(D', D) = (5.03 \times 10^6, 4.85 \times 10^6)$ Hz, Figs. 4(c) and 4(d) for medium tunneling rates $(D', D) = (5.03 \times 10^7, 4.85 \times 10^7)$ Hz, and Figs. 4(e) and 4(f) for high tunneling rates $(D', D) = (5.03 \times 10^8, 4.85 \times 10^8)$ Hz are obtained by five different methods: (i) the analytical formulas neglecting the QPC shot noise given in Ref. [25] (in thin solid line), (ii) the joint probability $P(I, J, t)$ obtained with the replacement of $(e^{ik} \rightarrow 1 + ik)$ (i.e., neglecting the QPC shot noise) and the Bayesian rules (in light blue dotted line), (iii) the joint probability $P(I, J, t)$ obtained without the approximation of $(e^{ik} \rightarrow 1 + ik)$ and the Bayesian rules (in red open triangles), (iv) the numerical method described in Sec. VID (in blue dots) and (v) the quantum trajectory method described in Sec. IV (in red open diamonds). As expected, the curves obtained by methods (i) and (ii) coincide and by methods (iii) and (iv) coincide for a given set of QPC

tunneling rates. They all approach to each other for the high QPC tunneling rate case in Figs. 4(e) and 4(f), then start to deviate from each other near the end points of $I = D$ and D' for the medium QPC tunneling rate case in Figs. 4(c) and 4(d) and differ significantly from each other for the low QPC tunneling rate case in Figs. 4(a) and 4(b). This is consistent with the observations of the joint current probability distribution discussed in Sec. VII A 1 and indicates that one can approximately neglect the QPC shot noise for the parameter set shown in Figs. 4(e) and 4(f) but cannot do so for the parameter set shown in Figs. 4(a) and 4(b). When the QPC shot noise is completely ignored, $\langle\langle J \rangle\rangle_c$ and $\langle\langle J^2 \rangle\rangle_c$ calculated by analytical solution are universal semicircles as a function of the current I , have a maximum at $I = (D + D')/2$ and equal to zero at $I = D, D'$ even though the SQD tunneling rates are asymmetric, i.e., $\gamma_L \neq \gamma_R$ [25]. But, when the QPC shot noise is not negligible, when QPC current $I = D, D'$, the SQD is no longer completely occupied or empty within the whole duration time t . As a result, the conditional SQD $\langle\langle J \rangle\rangle_c$ and $\langle\langle J^2 \rangle\rangle_c$ are not equal to zero at the end points $I = D, D'$ of the interval $I = [D, D']$. Furthermore, $\langle\langle J \rangle\rangle_c$ and $\langle\langle J^2 \rangle\rangle_c$ in this case become asymmetric for different γ_L and γ_R tunneling rates. At the QPC current $I = D$, the SQD in most of the duration time t is empty, while at the QPC current $I = D'$, the SQD in most of the duration time t is occupied. For the parameter $(\gamma_L, \gamma_R) = (160, 586)$ of Fig. 4, the SQD has a larger unconditional probability $\gamma_R/(\gamma_L + \gamma_R)$ of being empty than the probability $\gamma_L/(\gamma_L + \gamma_R)$ of being occupied. This leads to more switchings at $I = D'$ than at $I = D$ and thus results in larger conditional current cumulants $\langle\langle J \rangle\rangle_c$ and $\langle\langle J^2 \rangle\rangle_c$ at $I = D'$ than at $I = D$ with maximums occurring at $I > (D + D')/2$. The results become opposite if $\gamma_L > \gamma_R$ for which the SQD has a larger unconditional probability $\gamma_L/(\gamma_L + \gamma_R)$ of being occupied, leading to more switchings at $I = D$ than at $I = D'$. Thus, the conditional current cumulants $\langle\langle J \rangle\rangle_c$ and $\langle\langle J^2 \rangle\rangle_c$ at $I = D$ are larger than at $I = D'$ with maximums occurring at $I < (D + D')/2$. If $\gamma_L = \gamma_R$, the equal unconditional probability of being empty and being occupied makes the QPC shot-noise contribution symmetric with respect to $I = (D + D')/2$, resulting in symmetrical conditional current cumulants $\langle\langle J \rangle\rangle_c$ and $\langle\langle J^2 \rangle\rangle_c$ with maximums at $I = (D + D')/2$.

We also simulate 120 000 realizations of the conditional SQD occupation number $\langle n_2(t) \rangle_c$ and QPC currents by quantum trajectory method to calculate $\langle\langle J \rangle\rangle_c$ and $\langle\langle J^2 \rangle\rangle_c$. The quantum trajectory method is described in the next section.

B. Counting statistics by quantum trajectories

We describe how we obtain the conditional counting statistics using the quantum trajectory method. Take the case of SQD-QPC as an example. Using Eqs. (25) and (23), we can numerically simulate the evolutions of the conditional expectation value of the electron occupation number $\langle n_2 \rangle_c(t)$ on the QD as well as the measured conditional instantaneous QPC current record $I_c(t)$ in a single run of a realistic experiment as shown in Fig. 2(b). The time-average QPC current I in time t can be obtained by integrating the instantaneous QPC current $I_c(t)$ over time t . The average QD current J can be obtained by the number M of electrons transmitted

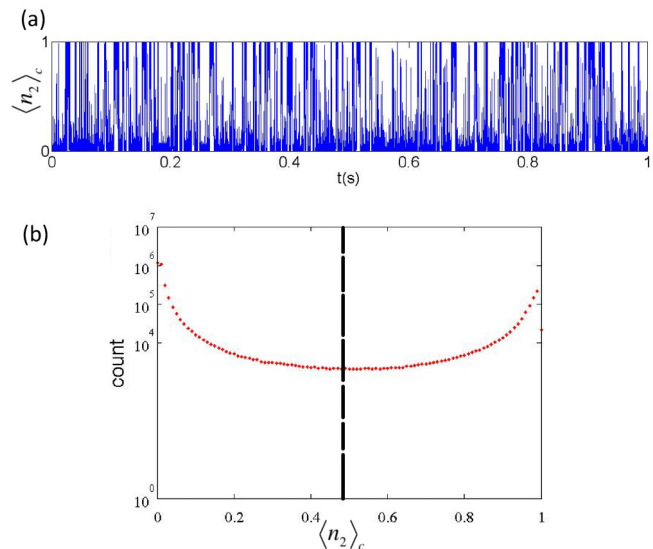


FIG. 5. (a) A simulated trajectory of $\langle n_2 \rangle_c$ for relatively moderate QPC tunneling rates of $(D, D', \gamma_L, \gamma_R) = (4.85 \times 10^7, 5.03 \times 10^7, 160, 586)$ Hz, i.e., with a moderate induced dephasing rate. (b) Histogram of each interval value of conditional $\langle n_2 \rangle_c$ for the trajectory shown in (a). The values from 0 to 1 for $\langle n_2 \rangle_c$ of the horizontal axis is divided into 101 intervals and the vertical axis of the number of counts is plotted on a logarithmic scale. The dashed line in the middle is the reference line of $\langle n_2 \rangle_c$.

through the QD in time t , i.e., $J = M/t$. The number M could be determined [25] by the number of “up” and then immediate “down” switches M of the random telegraph signal in a given time trace of $I_c(t)$ of duration t , or the number of “1” and then immediate “0” switches M in a given time trace $\langle n_2 \rangle_c(t)$ of duration t [see Fig. 2(a)]. When the strength of the random telegraph signal is much larger than that of the QPC intrinsic current (shot) noise [25], this provides an excellent way to determine the occupation number $\langle n_2 \rangle_c(t)$ on the QD and the average current J through the QD (even if the current J is rather weak). However, when the noise induced by the random telegraph signal is not much smaller than or is comparable to the QPC shot noise, the measured QPC current $I_c(t)$ may not be able to give an unambiguous measurement of the occupation number 1 or 0 on the QD. For example, a typical trace or realization of $\langle n_2 \rangle_c(t)$ for the parameter set of medium QPC tunneling rates of $(D', D) = (5.03 \times 10^7, 4.85 \times 10^7)$ Hz is shown in Fig. 5(a). Comparing the QPC current trace shown in Fig. 5(a) to that in Fig. 2(a) for the case of $(D', D) = (5.03 \times 10^{10}, 4.85 \times 10^{10})$ Hz with a large χ value, one finds that many values of $\langle n_2 \rangle_c(t)$ in the trajectory shown in Fig. 5(a) are close to or in-between but not at either 0 or 1 due to relatively large contribution from the shot-noise fluctuations. This leads to ambiguity in counting the number of electrons tunneling on and off dot 2 and then onto the right lead (or drain) with the method outlined in Ref. [25]. Therefore, we adopt a semiempirical method with details described in Appendix to diminish the ambiguity, to count the number M of electrons which have tunneled through dot 2 into the right lead of the QD system, and thus to obtain the average QD current $J = M/t$ for a given trajectory $\langle n_2 \rangle_c(t)$ in time t . Moreover, the corresponding

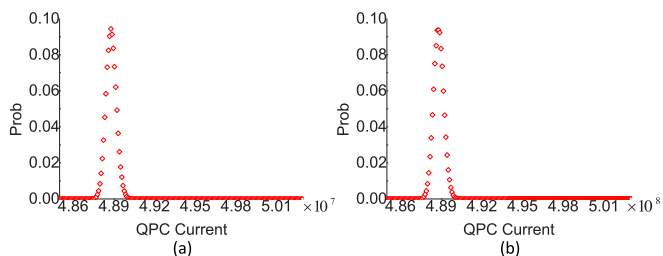


FIG. 6. Probability distributions of the QPC current (a) for the case presented in Figs. 4(c) and 4(d), and (b) for the case presented in Figs. 4(e) and 4(f). The whole range $[D, D']$ of the horizontal axis of the QPC current shown in (a) and in (b) is divided into 200 intervals.

average QPC current I in time t can be obtained by integrating the instantaneous QPC current of $I_c(t)$ generated from Eq. (23). Thus, we know both J and I of the given trajectory $\langle n_2 \rangle_c(t)$ in time t . We divide the values of $I(J)$ into small intervals. After simulating many trajectories to get meaningful statistics, we categorize the values of $I(J)$ extracted from the trajectories into their corresponding small intervals. To calculate the QD current cumulant $\langle\langle J \rangle\rangle_c$ conditioned on the QPC current I , we calculate the average of the different values of the QD currents J_i that all fall into the same small interval I_i (i.e., corresponding to the same value of I) as $\langle\langle J \rangle\rangle_c = \sum_{i=1}^S J_i / S$, where S is the number of samples J_i in this interval of I_i . The QD current noise cumulant $\langle\langle J^2 \rangle\rangle_c$ conditioned on the QPC current I is obtained by $\langle\langle J^2 \rangle\rangle_c = t[\sum_{i=1}^S J_i^2 / S - \langle\langle J \rangle\rangle_c^2]$.

The results of $\langle\langle J \rangle\rangle_c$ and $\langle\langle J^2 \rangle\rangle_c$ obtained by the quantum trajectory method with 120 000 realizations of $\langle n_2 \rangle_c(t)$ are shown in open diamonds in Figs. 4(c) and 4(d) and in Figs. 4(e) and 4(f) for different sets of (D, D') values. One notices that the results of the quantum trajectory method in Figs. 4(e) and 4(f) for large QPC tunneling rates or large $(D' - D)^2$ are in a better agreement with those of other methods than the results in Figs. 4(c) and 4(d) for small QPC tunneling rates or small $(D' - D)^2$. This is because larger difference of QPC tunneling rates or larger $(D' - D)^2$ represents a better occupation number measurement of dot 2 and a better condition to ignore the QPC shot noise, which in turn give a more accurate number M of electrons that have tunneled through dot 2 into the right lead of the QD system in time t for a given trajectory $\langle n_2 \rangle_c(t)$ and thus the corresponding average QD current $J = M/t$.

One also notices that the open diamonds representing $\langle\langle J \rangle\rangle_c$ and $\langle\langle J^2 \rangle\rangle_c$ obtained by the quantum trajectory method in Figs. 4(c) and 4(d) and in Figs. 4(e) and 4(f) show only results in certain ranges of the QPC currents, which should correspond to the regimes where the probability distributions of the QPC current $P(I)$ are not small. Indeed, the corresponding probability distributions $P(I) = \int P(I, J)dJ$ shown, respectively, in Figs. 6(a) and 6(b) are highly concentrated with appreciable values only in the same small ranges of the QPC currents I of their corresponding plots in Fig. 4. Consequently, even a large number of 120 000 quantum trajectories give only data samples in that small range of I . The first and last open diamonds in $\langle\langle J^2 \rangle\rangle_c$ of Fig. 4(f) deviate more from the results obtained by other methods due to the fact that the numbers of QD current data samples in the two corresponding QPC current intervals

are not large enough to give accurate statistics of conditional noise $\langle\langle J^2 \rangle\rangle_c$. We thus disregard the results of the QPC current intervals outside the regime bounded by the two intervals as less data samples are expected and observed.

In short, the quantum trajectory method can, in principle, give the full information about the transport properties provided a very large number of trajectories are available. However, due to highly concentrated QPC current probability distribution, a substantial amount of different realizations of quantum trajectories that can perhaps already simulate unconditional quantities well can still not sample the complete range of the QPC currents for the conditional quantities. Thus, an efficient method to calculate the conditional counting statistics is demanding, and the method that is also capable of treating more complicated nanostructure transport systems (e.g., the DQD-QPC system) described in Sec. VID provides exactly such a method.

C. DQD-QPC system

Electron transport properties through a DQD system have been studied intensively [15,16,27,39–45], Unconditional transport properties of a DQD system measured by a QPC have also been investigated [5,15,27–31]. Here, we concentrate on the conditional current cumulants through a DQD system conditioned on the observed average QPC current, which has not yet been explored extensively in the literature.

1. Conditional counting statistics

As mentioned, it is numerically unstable to follow the same procedure [25] of taking (partial) derivatives to find conditional current cumulants from Eqs. (65), (66), (67), and (68) for the DQD-QPC system. It is also numerically inefficient (using too much memory) to calculate the joint probability distribution (59), and then use the Bayesian formalism to find the conditional quantities for the DQD-QPC system.

Here, we use our numerically stable and efficient method to calculate $\langle\langle J \rangle\rangle_c$ and $\langle\langle J^2 \rangle\rangle_c$, and discuss their dependence on Ω and Γ_d . The dephasing rates Γ_d on the DQD's due to the QD-occupation-dependent QPC tunneling rates of $(D', D) = (5.03 \times 10^7, 4.85 \times 10^7)$ Hz and $(D', D) = (5.03 \times 10^8, 4.85 \times 10^8)$ Hz that will be considered are estimated from Eq. (39) to be about $\Gamma_d = 8200$ and $82\,000$ Hz, respectively. We will discuss cases with values of interdot coupling Ω greater than, smaller than, and comparable to Γ_d .

Considering the case of large $\Omega = 15\,000$ Hz, we compare the conditional cumulants $\langle\langle J \rangle\rangle_c$ and $\langle\langle J^2 \rangle\rangle_c$ of the DQD's to those of SQD with the same values of $\gamma_L = 160$ Hz and $\gamma_R = 586$ Hz as the DQD's. In Figs. 7(a) and 7(b) where $\Gamma_d = 8200$ Hz is smaller than $\Omega = 15\,000$ Hz, the agreement in $\langle\langle J \rangle\rangle_c$ and $\langle\langle J^2 \rangle\rangle_c$ between DQD's and SQD is rather good, indicating that the coherently coupled DQD's can be approximately regarded as a SQD. On the other hand, in Figs. 7(c) and 7(d), where $\Gamma_d = 82\,000$ Hz is larger than $\Omega = 15\,000$ Hz, there are appreciable differences between DQD and SQD results due to the effect of stronger dephasing (back-action) caused by the QPC. The larger Γ_d tends to reduce the coherent tunneling amplitude between the DQD's and hence reduce the current passing through the DQD's. As a

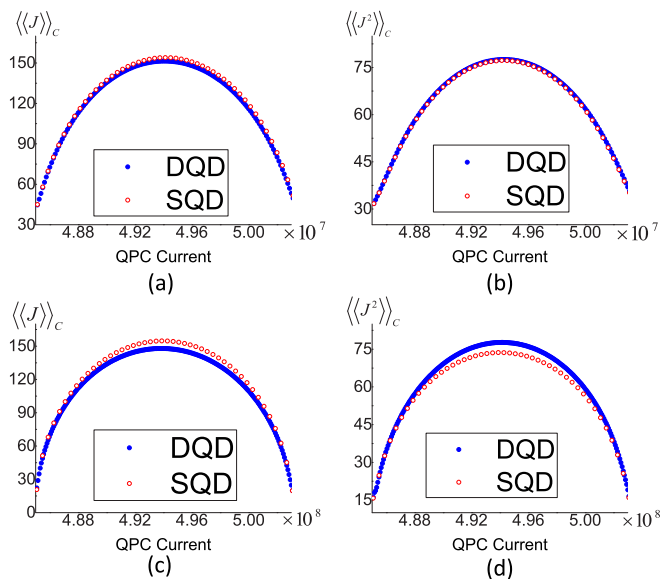


FIG. 7. Conditional DQD $\langle\langle J \rangle\rangle_c$ (left panel) and $\langle\langle J^2 \rangle\rangle_c$ (right panel) plotted as a function of the observed average QPC current I with high interdot coupling $\Omega = 15000$ Hz for (a) and (b) $(D', D) = (5.03 \times 10^7, 4.85 \times 10^7)$ Hz, and (c) and (d) $(D', D) = (5.03 \times 10^8, 4.85 \times 10^8)$ Hz. The DQD cumulants plotted in solid blue dots are compared with their SQD counterparts in open red dots with the same QD tunneling rates of $(\gamma_L, \gamma_R) = (160, 586)$ Hz from the left lead and to the right leads, respectively.

result, the value of the conditional current $\langle\langle J \rangle\rangle_c$ of the DQD-QPC system is slightly smaller than that of the SQD-QPC system [see Fig. 7(c)]. In contrast, the value of the conditional zero-frequency current noise $\langle\langle J \rangle\rangle_c$ of the DQD-QPC system is slightly larger than that of regarding the DQD system as a strongly coherently coupled SQD-QPC system [see Fig. 7(d)]. This is consistent with the unconditional noise property that quantum coherence suppresses noise [27,42,46].

In the low coherent tunneling regime where $\Omega \ll \Gamma_d$, the QPC charge detector introduces substantial decoherence to the DQD's. Thus, the dynamics of the electron transport of the coherent tunneling DQD's described by the (6×6) matrix $\mathcal{L}(k, q)$ defined in Eq. (38) can be in this case effectively described by a sequential tunneling (4×4) matrix defined in Eq. (41). This is clearly shown in Fig. 8 in which the condition $\Omega \ll \Gamma_d$ holds and the results of $\langle\langle J \rangle\rangle_c$ and $\langle\langle J^2 \rangle\rangle_c$ calculated by our numerical method with the coherent tunneling matrix of Eq. (38) and with the sequential tunneling matrix of Eq. (41) coincide. Also shown in red open squares are the results obtained by the quantum trajectory method, which are in good agreement with the results by our numerical method. However, only the results conditioned on small values of I_{QPC} are available due to small effective sequential tunneling rate Γ_Ω of Eq. (40). This then makes the second dot (the right dot) of the DQD's preferring to be empty, resulting in probability distribution of $P(I)$ concentrating in a small regime of the QPC currents I as shown in Figs. 9(a) and 9(b). This highlights the inability of the quantum trajectory method to cover in practice the whole range of the QPC current I for the cases of extremely small Γ_Ω .

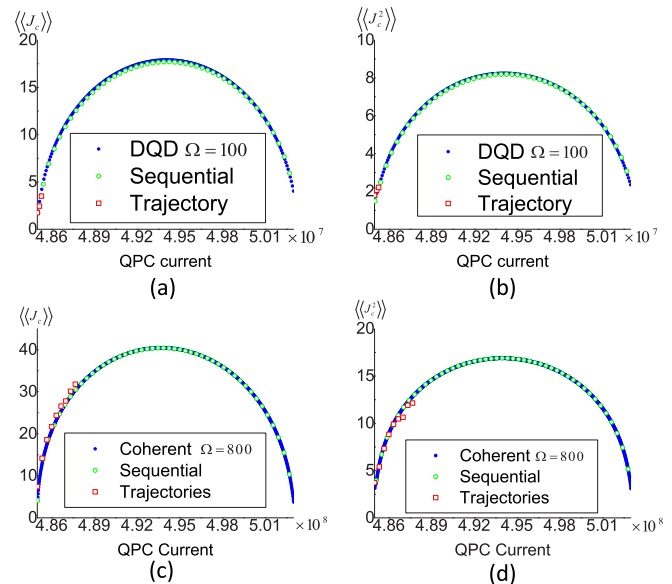


FIG. 8. Conditional DQD $\langle\langle J \rangle\rangle_c$ (left panel) and $\langle\langle J^2 \rangle\rangle_c$ (right panel) plotted as a function of the observed average QPC current I for different interdot couplings and QPC tunneling rates of (a) and (b) $(D', D, \Omega) = (5.03 \times 10^7, 4.85 \times 10^7, 100)$ Hz, and (c) and (d) $(D', D, \Omega) = (5.03 \times 10^8, 4.85 \times 10^8, 800)$ Hz obtained by the number-resolved master equations of coherent tunneling (in blue solid dots) and sequential tunneling (in open green dots) and by the method of quantum trajectories (in open red squares). The tunneling rates of the DQD's from the left lead and to the right leads are, respectively, $(\gamma_L, \gamma_R) = (160, 586)$ Hz.

However, when Ω , Γ_d , γ_L , and γ_R are comparable, using the classical master equation of the sequential tunneling matrix of Eq. (41) involving only the occupation probabilities cannot treat this case of the DQD system. The unconditional steady-state currents $\langle\langle J \rangle\rangle$ obtained by the unconditional master equation of sequential tunneling and the unconditional quantum master equation of coherent tunneling are the same independent of the DQD and QPC parameters [27,42,46]. But, the steady-state unconditional zero-frequency noise $\langle\langle J^2 \rangle\rangle$, in the parameter regime in which Ω , Γ_d , γ_L , and γ_R are all comparable [27,42,46], shows considerable difference between the coherent and the sequential tunneling cases. Choosing comparable parameters of interdot coupling $\Omega =$

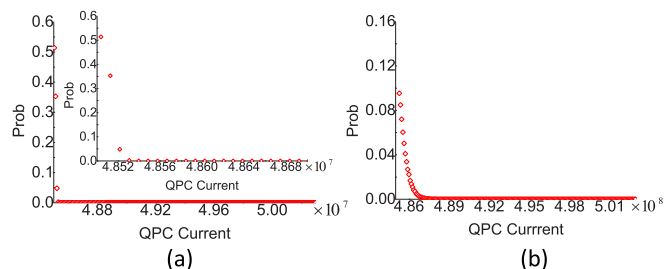


FIG. 9. Probability distributions of the QPC current (a) for the case presented in Figs. 8(a) and 8(b), and (b) for the case presented in Figs. 8(c) and 8(d). The inset in (a) is its zoom-in plot for small QPC currents. The whole range $[D, D']$ of the horizontal axis of the QPC current shown in (a) and in (b) is divided into 200 intervals.

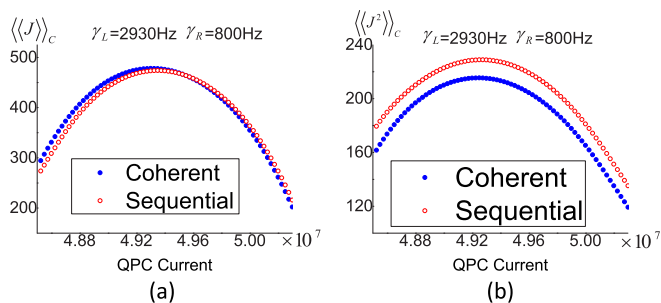


FIG. 10. Conditional DQD $\langle\langle J \rangle\rangle_c$ (left panel) and $\langle\langle J^2 \rangle\rangle_c$ (right panel) plotted as a function of the observed average QPC current I obtained by the number-resolved master equations of coherent tunneling (in blue solid dots) and sequential tunneling (in open red dots) with interdot coupling $\Omega = 3000$ Hz, QPC tunneling rates $(D', D) = (5.03 \times 10^7, 4.85 \times 10^7)$ Hz, and QD tunneling rates $(\gamma_L, \gamma_R) = (2930, 800)$ Hz.

3000 Hz, dephasing rate by the QPC $\Gamma_d = 8200$ Hz for the QPC currents $(D', D) = (5.03 \times 10^7, 4.85 \times 10^7)$ Hz, and the DQD tunneling rates from the left lead and to the right leads $(\gamma_L, \gamma_R) = (2930, 800)$ Hz, respectively, we show in Fig. 10 the conditional steady-state DQD current and zero-frequency noise for $\Delta\epsilon = 0$. One can see that the steady-state conditional currents $\langle\langle J \rangle\rangle_c$ obtained by the coherent-tunneling and sequential-tunneling master equations show still some observable difference, in contrast to no difference in their unconditional counterparts. The conditional steady-state noise $\langle\langle J^2 \rangle\rangle_c$ obtained by the coherent-tunneling master equation with the matrix of Eq. (38) is considerably smaller than that obtained by the sequential-tunneling master equation with the matrix of Eq. (41), i.e., quantum coherence suppresses noise as in the unconditional case [27,42,46].

The unconditional current moment can be expressed as $\langle J^r \rangle = \int_0^\infty dI P(I) \langle J^r \rangle_c$ and thus can be calculated from the conditional counting statistics. We thus use the conditional counting statistics obtained by our numerical method to compute unconditional current cumulants. The results are consistent with the unconditional current cumulants obtained by the method of Ref. [27]. Thus, conditional counting statistics can provide more detailed information about and physical insight into the quantum transport properties of the system than its unconditional counterpart.

VIII. CONCLUSION

We have applied the maximum eigenvalue method, the quantum trajectory method, and a stable and efficient method we develop to calculate the conditional counting statistics of QD systems measured by a QPC detector. The method we develop is capable of calculating the conditional counting statistics for a more complex system than the maximum eigenvalue method and for a wider range of parameters than the quantum trajectory method. We have investigated the effect of QPC shot noise on the conditional cumulants of the QD systems. For the considered case of high QPC tunneling rates for which the QPC shot noise as compared to the noise contribution of the random telegraph signal in the QPC current trace is small and can be neglected, our results are

in excellent agreement with those obtained by the method of Ref. [25]. However, for the cases of low QPC tunneling rates for which the QPC shot noise cannot be neglected, significant difference between $\langle\langle J \rangle\rangle_c$ and $\langle\langle J^2 \rangle\rangle_c$ obtained by our method and those obtained by the analytical solutions of Ref. [25] can be observed. We have also shown that for strong interdot coupling of $\Omega \gg \Gamma_d$, conditional DQD cumulants $\langle\langle J \rangle\rangle_c$ and $\langle\langle J^2 \rangle\rangle_c$ recover those of a SQD case (i.e., the DQD's act as a SQD). For small interdot coupling ($\Omega \ll \Gamma_d$), the results of $\langle\langle J \rangle\rangle_c$ and $\langle\langle J^2 \rangle\rangle_c$ calculated by our numerical method with the coherent-tunneling matrix and with the sequential-tunneling matrix coincide, while they show considerable difference when $\Omega, \Gamma_d, \gamma_L$, and γ_R are all comparable. The conditional current cumulants that are significantly different from their unconditional counterparts can provide additional information and insight into the electron transport properties of mesoscopic nanostructure systems.

ACKNOWLEDGMENTS

H.S.G. acknowledges support from the the Ministry of Science and Technology of Taiwan under Grants No. MOST 103-2112-M-002-003-MY3 and No. MOST 106-2112-M-002-013-MY3, from the National Taiwan University under Grant No. NTU-CCP-106R891703, and from the thematic group program of the National Center for Theoretical Sciences, Taiwan. We also acknowledge useful discussion with Dr. C.-H. Lin in the early stage of this work.

APPENDIX: SEMIEMPIRICAL METHOD TO COUNT THE ELECTRON TUNNELING EVENTS

The detailed procedure of the semiempirical method used to count the number of tunneling electrons in each of the quantum trajectories is described as follows. First, divide the entire range of values from 0 to 1 of $\langle n_2 \rangle_c(t)$ into several small intervals and count the numbers of $\langle n_2 \rangle_c(t)$ values that fall into each interval in a quantum trajectory (see Fig. 5). Second, select the interval where the value of histogram is minimum and let the middle value of $\langle n_2 \rangle_c(t)$ in this minimum interval as the reference value or line [as indicated in Fig. 5(b)] to determine whether the QD is occupied or empty. Third, calculate the average value of $\langle n_2 \rangle_c$ over the region on the left (right) side of the reference line and set it as the lower (upper) threshold whose value is usually close to 0 (1). Suppose the QD is initially being empty, the value of $\langle n_2 \rangle_c(t)$ is small. Then, the QD is considered being occupied only until $\langle n_2 \rangle_c(t)$ is above the upper threshold; the QD is considered being empty again only until $\langle n_2 \rangle_c(t)$ is below the lower threshold. Thus, when $\langle n_2 \rangle_c(t)$ in a quantum trajectory realization reaches the above occupied situation and then the immediate empty situation sequentially and successively, an electron tunneling event from the QD to the right lead is registered. By this counting method, we can obtain the number M of electrons that have tunneled through the QD system. With this counting method, one can proceed to calculate the conditional current cumulants as described in Sec. VII B.

- [1] J. M. Elzerman, R. Hanson, L. H. Willems van Beveren, B. Witkamp, L. M. K. Vandersypen, and L. P. Kouwenhoven, *Nature (London)* **430**, 431 (2004).
- [2] R. Schleser, E. Ruh, T. Ihn, K. Ensslin, D. C. Driscoll, and A. C. Gossard, *Appl. Phys. Lett.* **85**, 2005 (2004).
- [3] L. M. K. Vandersypen, J. M. Elzerman, R. N. Schouten, L. H. Willems van Beveren, R. Hanson and L. P. Kouwenhoven, *Appl. Phys. Lett.* **85**, 4394 (2004).
- [4] S. Gustavsson, R. Leturcq, B. Simović, R. Schleser, T. Ihn, P. Studerus, K. Ensslin, D. C. Driscoll, and A. C. Gossard, *Phys. Rev. Lett.* **96**, 076605 (2006).
- [5] S. Gustavsson, R. Leturcq, M. Studer, I. Shorubalko, T. Ihn, K. Ensslin, D. C. Driscoll, and A. C. Gossard, *Surf. Sci. Rep.* **64**, 191 (2009).
- [6] N. Ubbelohde, C. Fricke, C. Flindt, F. Hohls, and R. J. Haug, *Nat. Commun.* **3**, 612 (2012).
- [7] W. Lu, Z. Ji, L. Pfeiffer, K. W. West, and A. J. Rimberg, *Nature (London)* **423**, 422 (2003).
- [8] T. Fujisawa, T. Hayashi, Y. Hirayama, H. D. Cheong, and Y. H. Jeong, *Appl. Phys. Lett.* **84**, 2343 (2004).
- [9] J. Bylander, T. Duty, and P. Delsing, *Nature (London)* **434**, 361 (2005).
- [10] T. Fujisawa, T. Hayashi, R. Tomita, and Y. Hirayama, *Science* **312**, 1634 (2006).
- [11] C. Fricke, F. Hohls, W. Wegscheider, and R. J. Haug, *Phys. Rev. B* **76**, 155307 (2007).
- [12] L. S. Levitov and G. B. Lesovik, *Pis'ma Zh. Eksp. Teor. Fiz.* **58**, 225 (1993) [*JETP Lett.* **58**, 230 (1993)]; L. S. Levitov, H. W. Lee, and G. B. Lesovik, *J. Math. Phys.* **37**, 4845 (1996).
- [13] D. A. Bagrets and Yu. V. Nazarov, *Phys. Rev. B* **67**, 085316 (2003).
- [14] *Quantum Noise in Mesoscopic Physics*, edited by Y. V. Nazarov (Springer, London, 2003).
- [15] S. A. Gurvitz, *Phys. Rev. B* **56**, 15215 (1997).
- [16] H. Sprekeler, G. Kießlich, A. Wacker, and E. Schöll, *Phys. Rev. B* **69**, 125328 (2004).
- [17] S.-K. Wang, H. Jiao, F. Li, X.-Q. Li, and Y. J. Yan, *Phys. Rev. B* **76**, 125416 (2007).
- [18] G. Schaller, G. Kiesslich, and T. Brandes, *Phys. Rev. B* **80**, 245107 (2009).
- [19] C. Flindt, T. Novotný, A. Braggio, and A.-P. Jauho, *Phys. Rev. B* **82**, 155407 (2010).
- [20] A. N. Korotkov, *Phys. Rev. B* **63**, 085312 (2001); **60**, 5737 (1999).
- [21] H.-S. Goan, G. J. Milburn, H. M. Wiseman, and H. B. Sun, *Phys. Rev. B* **63**, 125326 (2001).
- [22] H.-S. Goan and G. J. Milburn, *Phys. Rev. B* **64**, 235307 (2001).
- [23] H.-S. Goan, *Quantum Inf. Comput.* **3**, 121 (2003).
- [24] H.-S. Goan, *Phys. Rev. B* **70**, 075305 (2004).
- [25] E. V. Sukhorukov, A. N. Jordan, S. Gustavsson, R. Leturcq, T. Ihn, and K. Ensslin, *Nat. Phys.* **3**, 243 (2007).
- [26] A. N. Jordan and E. V. Sukhorukov, *Phys. Rev. Lett.* **93**, 260604 (2004).
- [27] G. Kießlich, P. Samuelsson, A. Wacker, and E. Schöll, *Phys. Rev. B* **73**, 033312 (2006).
- [28] J. R. Petta, A. C. Johnson, C. M. Marcus, M. P. Hanson, and A. C. Gossard, *Phys. Rev. Lett.* **93**, 186802 (2004).
- [29] J. Gorman, D. G. Hasko, and D. A. Williams, *Phys. Rev. Lett.* **95**, 090502 (2005).
- [30] S. H. Ouyang, C. H. Lam, and J. Q. You, *Phys. Rev. B* **81**, 075301 (2010).
- [31] D. S. Golubev, Y. Utsumi, M. Marthaler, and G. Schön, *Phys. Rev. B* **84**, 075323 (2011).
- [32] A. Shnirman and G. Schön, *Phys. Rev. B* **57**, 15400 (1998).
- [33] Y. Makhlin, G. Schön, and A. Shnirman, *Phys. Rev. Lett.* **85**, 4578 (2000); *Rev. Mod. Phys.* **73**, 357 (2001).
- [34] J. Li, Y. Liu, J. Ping, S. S. Li, X. Q. Li, and Y. J. Yan, *Phys. Rev. B* **84**, 115319 (2011).
- [35] C. Flindt, T. Novotný, and A.-P. Jauho, *Phys. Rev. B* **70**, 205334 (2004).
- [36] C. Flindt, T. Novotný, and A.-P. Jauho, *Europhys. Lett.* **69**, 475 (2005).
- [37] C. Flindt, T. Novotný, A. Braggio, M. Sassetti, and A.-P. Jauho, *Phys. Rev. Lett.* **100**, 150601 (2008).
- [38] N. Lambert, C. Flindt, and F. Nori, *Europhys. Lett.* **103**, 17005 (2013).
- [39] W. G. van der Wiel, S. De Franceschi, J. M. Elzerman, T. Fujisawa, S. Tarucha, and L. P. Kouwenhoven, *Rev. Mod. Phys.* **75**, 1 (2002).
- [40] S. A. Gurvitz and Y. S. Prager, *Phys. Rev. B* **53**, 15932 (1996); S. A. Gurvitz, *ibid.* **57**, 6602 (1998).
- [41] M. R. Wegewijs and Y. V. Nazarov, *Phys. Rev. B* **60**, 14318 (1999).
- [42] H. B. Sun and G. J. Milburn, *Phys. Rev. B* **59**, 10748 (1999).
- [43] J. Y. Luo, H. J. Jiao, Y. Shen, G. Cen, X.-L. He, and C. Wang, *J. Phys.: Condens. Matter* **23**, 145301 (2011).
- [44] T. Hayashi, T. Fujisawa, H. D. Cheong, Y. H. Jeong, and Y. Hirayama, *Phys. Rev. Lett.* **91**, 226804 (2003).
- [45] R. Ziegler, C. Bruder, and H. Schoeller, *Phys. Rev. B* **62**, 1961 (2000).
- [46] R. Aguado and T. Brandes, *Phys. Rev. Lett.* **92**, 206601 (2004).